ON THE CHEMICAL COMPOSITION OF SEPIOLITE AND PALYGORSKITE

E. García-Romero[1,*] and M. Suárez[2]

[1] Departamento de Cristalografía y Mineralogía, Facultad de Ciencias Geológicas, Universidad Complutense, Madrid, Spain
[2] Departamento de Geología, Universidad de Salamanca, Plaza de la Merced s/n, 37008 Salamanca, Spain

Abstract—Many studies of the chemical composition of sepiolite and palygorskite have been carried out using analytical electron microscopy (AEM). According to the literature, a compositional gap exists between sepiolites and palygorskites, but the results presented here show that they may all be intermediate compositions between two extremes. The results of >1000 AEM analyses and structural formulae have been obtained for the samples studied (22 samples of sepiolite and 21 samples of palygorskite) and indicate that no compositional gap exists between sepiolite and palygorskite. Sepiolite occupies the most magnesic and trioctahedral extreme and palygorskite the most aluminic-magnesic and dioctahedral extreme. Sepiolite and palygorskite with intermediate compositions exist between the two pure extremes: (1) sepiolite with a small proportion of octahedral substitution; (2) palygorskite with a very wide range of substitution (the pure dioctahedral extreme is unusual); and (3) intermediate forms, Al-sepiolite and Mg-palygorskite with similar or the same chemical composition. The chemical compositions of the intermediate forms can be so similar that a certain degree of polymorphism exists between Al-sepiolite and Mg-palygorskite.

Key Words—Chemical Composition, Octahedral Sheet, Octahedra cations, Palygorskite, Sepiolite.

INTRODUCTION

The sepiolite and palygorskite group of clay minerals has been studied extensively because they make up a very important group of minerals with a huge number of industrial applications. The number of chemical analyses which have been carried out is small, however, and many of the chemical data reported in the literature are the result of bulk-rock analyses and can be affected by other clay minerals and other associated minerals as impurities. Published results of microanalyses of individual particles of both sepiolite and palygorskite are quite rare.

According to the literature, a compositional gap exists between the extremes of these fibrous clay minerals. The trioctahedral extreme is sepiolite and the more dioctahedral extreme, palygorskite (Martín-Vivaldi and Fenoll, 1970; Paquet *et al.*, 1987; Galán and Carretero, 1999). The structure of both sepiolite and palygorskite contains ribbons of 2:1 phyllosilicates linked by periodic inversion of the apical oxygen of the continuous tetrahedral sheet every six atoms of Si (three tetrahedral chains) for sepiolite and every four atoms of Si (two tetrahedral chains) for palygorskite. Ribbons (referred to as 'polisomes' by Krekeler and Guggenheim, 2008) extend parallel to the axis of the fiber. The tetrahedral sheet is continuous across ribbons but the octahedral sheet is discontinuous as a result of the periodic inversion, and terminal octahedral cations must complete their coordination sphere with water molecules referred to as coordinated water. Sepiolite has eight possible octahedral positions per half unit cell (p.h.u.c.); all are occupied and its structural formula is $Si_{12}O_{30}Mg_8(OH)_4(OH_2)_2{\cdot}4H_2O$ (Brauner and Preisinger, 1956). The number of octahedral positions (p.h.u.c.) in palygorskite is five, $Si_8O_{20}Mg_5(OH)_2(OH_2)_4{\cdot}4H_2O$ according to the structure proposed by Bradley (1940), although the five positions cannot be filled (Serna *et al.* 1977) and a dioctahedral mineral with a structural formula $Si_8O_{20}Al_2Mg_2(OH)_2(OH_2)_4{\cdot}4H_2O$ is accepted.

Since the earliest articles published on the chemical composition of the two minerals, the possibility of a continuous series between sepiolite and palygorskite had been postulated but also ruled out: "In nature no evidence is apparent for a continuous solid solution series between the two, although this may be expected from the postulated similarity of their structures" (Mumpton and Roy, 1958).

Various authors have studied the chemical composition of sepiolite and palygorskite and they fixed compositional limits. Martín-Vivaldi and Cano-Ruíz (1956) suggested that the minerals of the palygorskite sepiolite group occupy the region of discontinuity between dioctahedral and trioctahedral minerals. Brauner and Presinger (1956) reported that the number of octahedral cations for bulk analyses for sepiolite ranges between 6.95 and 8.11 for eight octahedral positions and that ^{VI}Mg varies between 4.96 and 8.1. For palygorskite, Drits and Sokoleva (1971) established that the sum of octahedral cations for bulk analyses ranges from 3.45 to 4.33 with ^{VI}(Al+Fe) between 1.12 and 2.3 for five octahedral positions. Paquet *et al.* (1987) studied 145 individual particles from palygorskite-smectite and sepiolite-smectite assemblages and affirmed that the octahedral composition fields of the

smectites and fibrous clays partly overlap. The sepiolite field is clearly in the trioctahedral domain, whereas the palygorskite field is both in the dioctahedral as well as between the trioctahedral and dioctahedral domains. Newman and Brown (1987) confirmed that the total number of octahedral cations of sepiolite ranges from 7.01 to 8.01 and between 3.76 and 4.64 for palygorskite, with a mean value of 4.00. Galán and Carretero (1999) published another approach to compositional limits for sepiolite and palygorskite and concluded that sepiolite is a true trioctahedral mineral, with negligible structural substitutions and eight octahedral positions filled with Mg, while palygorskite is intermediate between di- and trioctahedral phyllosilicates and its octahedral sheet contains mainly Mg, Al, and Fe(III) with an R2/R3 (where R2 = ΣM(II), R3 = ΣM(III)) ratio close to 1 and four of the five structural positions occupied. Minor Mn(II), Fe(II), or Ni is also possible in octahedral positions. If Ni > Mg, the species is named falcondoite (Springer, 1976; Taulet *et al.*, 2009). Loughlinite is the Na-sepiolite, in which Mg is partially replaced by Na and also contains Na in the channels (Fahey and Axerod, 1948). Kadir *et al.* (2002) found authigenic loughlinite together with sepiolite in a Neogene volcano-sedimentary lacustrine environment in Mihaliççik-Eskişehir, Turkey. García-Romero *et al.* (2004) reported a very Mg-rich palygorskite with 4.36 octahedral cations (p.h.u.c.); Gionis *et al.* (2006) reported a very Fe-rich palygorskite; and Garcia-Romero *et al.* (2007) suggested, from AEM, that Al-rich sepiolite exists in the Allou-Kagne deposit. In addition, Suarez and García-Romero (2006) reported that isomorphic substitutions in octahedral palygorskite sheets occur only in *M*2 positions. Fe may occupy *M*2 positions whereas Mg can occupy all possible sites: *M*1, *M*2, and *M*3. In relation to the chemical composition of palygorskites, Suarez *et al.* (2006, 2007) proposed a classification into three types, and their relationship with d_{200} offering the possibility of examining the octahedral composition of a palygorskite sample using X-ray diffracton (XRD).

Most of the structural formulae reported in the literature are summarized here and a large number of analyses of individual particles of both sepiolite and palygorskite from different localities has been carried out, obtaining representative structural formulae, with the aim of establishing the compositional limit between the two minerals.

MATERIALS AND METHODS

Materials

The samples studied in the present work (22 samples of sepiolite and 21 samples of palygorskite) came from different localities around the world (Table 1). They show different textural features, with fibers which range from <1 μm to centimeters in length, and are of different geological origins, from sedimentary to hydrothermal rocks. All the samples were of high purity, although in some cases may contain small amounts of other minerals as impurities. Samples were either supplied by commercial enterprises in the case of ore deposits, collected by the authors, or came from specialized collectors. Some

Table 1. Sample sources.

Sepiolite		Palygorskite	
Sample	Location	Sample	Location
BAT	Batallones (Spain)	BER	Bercimuel (Spain)
BOS	Bosnia	BOA	Boavista (Brasil)
FIN	Finland	CAS	Cassiar (Canada)
GRA	Grant County (USA)	E10	Esquivias (Spain)
HEN	Henan (China)	E11	Esquivias (Spain)
HUN	Hunan (China)	GER	Geraldton (Australia)
LIE	Lieyang (China)	LIB	Lisboa (Portugal)
MAR	Mara (Spain)	LIL	Lisboa (Portugal)
MER	Eskişehir (Turkey)	MET	Metaline (USA)
MON	Monferrato (Italy)	NIJ	Níjar (Spain)
NAM	Namibia	OKE	Okehampton (UK)
NEI	Neixiang (China)	PAL	Palygorskaya (Russia)
NEV	Nevada (USA)	PIC	Pics Crossing (Australia)
NOR	Norway	SEG	Segovia (Spain)
POL	Polatli (Turkey)	TOR	Torrejón (Spain)
TPO	Polatli (Turkey)	TRA	Los Trancos (Spain)
SAN	Santa Cruz (USA)	Y0	Yucatán (México)
SOM	Somalia	Y1A	Yucatán (México)
VAL	Vallecas (Spain)	Y3	Yucatán (México)
VIC	Vicálvaro (Spain)	Y7	Yucatán (México)
XIX	Xixia (China)	Y8	Yucatán (México)
YUN	Yunclillos (Spain)		

Table 2. Structural formulae of sepiolites taken from the literature.

	Si	^{IV}Al	Fe^{3+}	Στ	^{VI}Al	Fe(III)	Fe(II)	Ti	Mg	Cr	Ni	Mn	Cu	Σo	Ca	K	Na	NH^{4+}	Cu
1	11.81	0.16	0.03	12.00		0.47	0.13		7.14					7.74	0.11				
2	11.61	0.22	0.12	11.95					7.35			0.52	0.14	8.01					
3	11.84	0.07	0.07	11.98					7.89					7.89	0.13	0.01	0.15		
4	11.95	0.05		12.00	0.01	0.07			7.89					7.97	0.20				
5	11.77	0.23		12.00	0.02	0.25	0.16		6.98			0.55		7.96		0.01			
6	11.78	0.22		12.00	0.06	0.01			7.89					7.96	0.12				
7	11.23	0.24	0.53	12.00		2.40	0.27		4.28			0.06		7.01	0.17				
8	11.38	0.10	0.52	12.00		2.27	0.12		4.67			0.03		7.09	0.10				
9	11.54	0.46		12.00	1.37	0.37	0.44		4.95					7.13					
10	11.96	0.04		12.00	0.17	0.46	0.26		6.78					7.67	0.03		0.03		
11	11.82	0.10	0.08	12.00					7.73					7.73	0.08	0.03	0.51		
12	11.93	0.07		12.00	0.01	0.03			7.96					8.00			0.03		
13	11.67	0.22	0.11	12.00					7.39			0.53		7.92					0.13
14	11.78	0.22		12.00	0.05	0.01			7.90					7.96	0.13				
15	11.87		0.13	12.00		0.03			7.90					7.93	0.13				
16	11.80	0.16	0.04	12.00		0.45	0.14		7.19					7.78	0.11				
17	11.68	0.24	0.08	12.00		0.53	0.13		7.24					7.90					
18	11.63	0.37		12.00	1.47	0.37			4.98					6.82					
19	11.70	0.26	0.04	12.00	0.06			0.02	7.60					7.68		0.16	0.26		
20	11.64	0.36		12.00	1.49	0.37	0.44		4.95					7.25				0.45	
21	11.84	0.16		12.00	0.79	0.12			6.04					6.95	0.09	0.36	0.24		
22	11.96	0.04		12.00	0.40	0.10			7.04					7.54	0.11	0.01	0.10		
23	12.01			12.01	0.05	0.05			7.32					7.42	0.46		0.05		
24	11.80	0.11	0.09	12.00		0.37			7.51					7.88	0.05				
25	11.62	0.38		12.00	0.04	0.06		0.02	7.72					7.84	0.16	0.13	0.08		
26	11.78	0.22		12.00	0.41	0.08			6.94					7.43	0.32	0.13	0.11		
27	11.58	0.42		12.00	0.11	0.13			7.53					7.77	0.19	0.11	0.13		
28	12.02			12.02	0.47	0.07		0.02	6.89					7.45	0.11	0.16	0.12		
29	11.88	0.12		12.00	0.29	0.08			7.36					7.73	0.12		0.05		
30	11.75	0.21		11.96					8.11					8.11		0.06	0.08		
31	11.28	0.72		12.00	0.05	0.26			7.44					7.75	0.21		0.51		
32	11.96	0.04		12.00	0.20	0.10		0.01	7.44					7.75	0.05	0.07	0.02		
33	12.05			12.05	0.05	0.01			7.78					7.84	0.03				
34	11.99	0.01		12.00	0.68	0.12		0.01	6.45					7.26	0.09	0.25	0.22		
35	11.72	0.28		12.00	0.48	0.15		0.04	6.50					7.17	0.22	0.25	0.51		
36	12.16			12.16	0.02	0.02	0.01		7.28					7.33		0.01			
37	11.95	0.05		12.00	0.10		0.06		7.76					7.92	0.03	0.06			
38	11.38	0.52	0.10	12.00		0.06	0.01	0.03	7.89					7.99	0.05	0.26	0.18		
39	11.83	0.08	0.08	11.99					7.90					7.90	0.13		0.15		
40	11.95	0.05		12.00		0.08			7.69					7.77	0.21				
41	11.49	0.33	0.18	12.00		0.37		0.03	7.61					8.01		0.01	0.01		
42	12.00			12.00	0.16	0.36		0.02	6.99	0.07	0.04			7.64	0.03	0.02	0.02		

Table 2 (*contd*)

	Si	^{IV}Al	Fe^{3+}	Στ	^{VI}Al	Fe(III)	Fe(II)	Ti	Mg	Cr	Ni	Mn	Cu	Σo	Ca	K	Na	NH^{4+}	Cu
43	11.99	0.01		12.00	0.06	0.02			7.84		0.03			7.95		0.01	0.01		
44	11.80	0.20		12.00	0.16	1.66			6.05					7.87	0.09		0.07		
45	12.05			12.05	0.05				7.56					7.61		0.02	0.24		
46	11.49	0.11		11.60					7.73					7.73	1.02	0.13	0.08		
47	12.04			12.04					7.93					7.93					
48	12.00			12.00					7.98					7.98					
49	12.03			12.03					7.94					7.94					
50	11.78	0.22		12.00	0.06	0.01			7.89					7.96	0.12				
51	11.80	0.16	0.04	12.00		0.47	0.13		7.14					7.74	0.11				
52	11.54	0.46		12.00	1.37	0.37	0.44		4.95					7.13				0.45	
53	11.96	0.04		12.00	0.17	0.46	0.26		6.78					7.67			0.03		
54	11.64	0.36		12.00	0.91	0.32			6.01					7.24	0.09	0.07			
55	11.89	0.11		12.00	0.38	0.19		0.04	6.88					7.49	0.21	0.06			
56	11.91	0.09		12.00	0.73	0.23		0.03	6.06					7.05	0.45	0.05			
57	11.81	0.19		12.00	0.67	0.25		0.02	6.32					7.26	0.25	0.06			
58	11.76	0.09		11.85		0.01		0.01	8.00					8.02		0.07	0.01		
59	11.42	0.46		11.88		0.31		0.05	7.67					8.03		0.06	0.03		
60	11.60	0.40		12.00		0.45		0.05	7.29					7.79		0.08	0.02		
61	12.00			12.00		0.10		0.02	7.09					7.21		0.07	0.03		
62	12.00			12.00		0.08		0.01	7.83					7.92		0.05	0.02		
63	12.00			12.00		0.04			7.82					7.86		0.07	0.01		
64	12.00			12.00		0.02			7.71					7.73		0.06	0.01		
65	11.91	0.09		12.00		0.05		0.01	7.80					7.86	0.05	0.06	0.04		
66	11.76	0.21	0.03	12.00		0.05		0.02	7.88					7.95		0.13	0.09		
67	12.00			12.00		0.04		0.01	7.60					7.65		0.06	0.02		
68	12.00			12.00	0.02	0.15		0.01	7.45			0.05		7.68	0.12	0.02	0.05		
69	11.98	0.02		12.00	0.06	0.42		0.01	6.75			0.05		7.29	0.40	0.03	0.11		
70	11.72	0.28		12.00	0.07	0.06		0.01	7.67			0.01		7.82	0.19	0.06	0.01		
71	12.00			12.00	0.06	0.02		0.01	7.39			0.01		7.49	0.07	0.02	0.04		
72	11.69	0.31		12.00	0.52	0.11		0.03	6.71			0.01		7.38	0.17	0.26	0.27		
73	11.87	0.13		12.00	0.18	1.66		0.01	5.22			0.01		7.08	0.08	0.01	0.01		
74	12.00			12.00	0.60	0.01		0.01	6.71			0.01		7.34	0.04	0.01	0.04		
75	12.00			12.00	0.39	0.09		0.01	6.92			0.01		7.42	0.02	0.12	0.02		
76	11.80	0.20		12.00	0.44	0.17		0.01	6.81			0.01		7.44	0.35	0.17	0.04		
77	12.00			12.00	0.08	0.02		0.01	7.46			0.01		7.58	0.04	0.01	0.07		
78	12.00			12.00		0.01			8.00					8.01					
79	11.79	0.21		12.00	0.02	0.23	0.16		6.99			0.56		7.96	0.12				
80	11.79	0.21		12.00	0.06	0.01			7.89					7.96					
81	12.01			12.01	0.03	1.75		0.01	6.05			0.02		7.86	0.06	0.02	0.08		
82	11.81	0.11	0.08	12.00		0.37			7.49					7.86	0.05				
83	11.48	0.51		11.99	0.26	1.54	0.30		4.45			0.15		6.70	0.19	0.69	0.77		
84	11.74	0.23		11.97	0.16	1.65			6.13			0.02		7.96	0.03	0.04	0.25		
85	11.92	0.08		12.00	0.27	0.01			7.56		0.02			7.86	0.04				

86	11.94	0.06		12.00	0.25	0.00			7.60		0.02		7.87	0.04			
87	11.99	0.01		12.00	0.06	0.02			7.84		0.03		7.95		0.01	0.01	
88	11.96	0.04		12.00	0.12	0.32			7.19		0.04		7.67	0.03	0.02	0.02	
89	11.60	0.24	0.16	12.00		0.10	0.08		7.55			0.27	8.00				
90	11.92	0.08		12.00	0.54	0.02	0.08		6.98				7.62		0.16	0.12	
91	11.89	0.11		12.00	0.15	0.08			7.31				7.55				
92	11.29	0.71		12.00	0.17	0.08		0.02	6.61			0.01	6.89	0.11	0.05	0.04	
93	11.38	0.62		12.00	0.23	0.41		0.05	6.94				7.63	0.11	0.18	0.24	
94	11.16	0.65	0.19	12.00		0.23		0.04	6.90				7.17	0.03	0.19	1.94	
95	12.00			12.00	0.42	0.09			7.00				7.51	0.11	0.15	0.12	
96	11.66	0.34		12.00	0.11	0.22			7.11			0.11	7.55	0.34			
97	11.72	0.28		12.00	0.06	0.04			7.96				8.00	0.04			

1–10 compiled by Newman and Brown (1987); 11–46 compiled by Galán and Carretero (1999); 47–49 from Galán and Carretero (1999); 50–53 compiled by Jones and Galán (1991); 54–57 from Zanbouh *et al.* (2005); 58–67 from Torres-Ruiz *et al.* (1994); 68–77 from López-Galindo and Sanchez Navas (1989); 78–84 from Imai and Otsuka (1984); 85–88 from Yalçin and Bozkaya (2004); 89–90 from Serna *et al.* (1977); 91 from Singer *et al.* (1998); 92 from Kadir *et al.* (2002); 92 from Akbulut and Kadir (2003); 93–94 from Kadir *et al.* (2002); 95 from Santaren *et al.* (1990); 96 from Arnuzo Perez *et al.* (1989); 97 from Chahi *et al.* (1997).

palygorskites were studied previously by the authors, with different aims, and partial results have already been published. In such cases, their structural formulae proposed here have been reviewed with the new data in mind.

Most of the sepiolite and palygorskite formulae from the literature have been collected (Tables 2, 3). These analyses show great variability having been obtained from different authors and analyzed by different techniques, including bulk chemical analyses of rocks, which could contain admixtures of other minerals as impurities which are difficult to separate.

Methods

The high purity of the samples was checked by X-ray diffraction using a Siemens D 500 XRD diffractometer with CuKα radiation and a graphite monochromator. The samples used were random-powder specimens. Powders were scanned over the range 2–65°2θ at a scan speed of 0.05°2θ/3 s to determine the mineralogical composition.

The chemical composition was obtained by analytical electron microscopy (AEM) with transmission electron microscopy (TEM), from samples of great purity. In order to ensure the reproducibility of the data, the analyses were carried out at two different laboratories: CAI of Electron Microscopy 'Luis Bru' (Complutense University, Madrid, Spain) and at the CIC (University of Granada, Spain). At CAI, the data were obtained using a JEOL 2000 FX microscope equipped with a double-tilt sample holder (up to a maximum of ±45°) at an acceleration voltage of 200 kV, with 0.5 mm zeta-axis displacement and 0.31 nm point-to-point resolution. The microscope incorporates an OXFORD ISIS energy dispersive X-ray spectrometer (136 eV resolution at 5.39 keV) and has its own software for quantitative analysis. At the CIC (University of Granada), a Philips CM-20 microscope operated at 200 kV (fitted with an ultrathin window, solid-state Si(Li) detector for energy dispersive X-ray analysis (EDAX)) was used. The atomic percentages were calculated by the Cliff-Lorimer thin-film ratio criteria (Lorimer and Cliff, 1976). The TEM observations were performed by depositing a drop of diluted suspension on a microscopic grid with collodion.

The structural formulae for all analysed particles were calculated on the basis of $O_{20}(OH)_2$ for palygorskites and $O_{30}(OH)_4$ for sepiolites. All the Fe present was considered as Fe(III) (owing to the limitation of the technique), but the possible existence of Fe(II) cannot be excluded.

RESULTS

The study of 22 samples of sepiolite and 21 of palygorskite by AEM generated >1000 analyses. Usually, a small number of the analyses obtained (~5%) are erroneous as a consequence of instrumental errors. Although they are AEM analyses, the influence of some impurities, specifically silica or cations adsorbed,

Table 3. Structural formulae of palygorskite taken from the literature.

	Si	^{IV}Al	Στ	^{VI}Al	Fe(III)	Fe(II)	Mg	Ti	Fe(II)	Mn	Ca	Σo	Ca	K	Na
1	7.34	0.66	8.00	2.25	0.17		1.47					3.89	0.21		
2	7.75	0.25	8.00	2.35	0.17		1.29					3.81	0.06		
3	7.61	0.39	8.00	2.26	0.23		1.43					3.92	0.02		
4	7.71	0.29	8.00	2.00	0.01		1.70					3.71		0.08	0.08
5	7.50	0.50	8.00	1.62	0.41		1.78					3.81	0.34		
6	8.06	0.00	8.06	2.00	0.05		1.62					3.67	0.08	0.01	0.04
7	7.80	0.20	8.00	1.51	0.38		2.22					4.11		0.09	
8	7.82	0.18	8.00	1.57	0.20		2.04					3.81	0.36		
9	8.09	0.00	8.09	1.57	0.00		2.24					3.81	0.12	0.14	0.07
10	7.88	0.12	8.00	0.95	0.42		2.81	0.10				4.28			
11	7.75	0.25	8.00	0.12	0.10	0.47	3.84	0.08				4.61	0.17	0.04	0.21
12	7.71	0.29	8.00	1.43	0.56		2.10					4.09			
13	7.86	0.14	8.00	1.84	0.40		1.71					3.95			
14	8.05	0.00	8.05	1.46	0.41		2.09					3.96			
15	7.81	0.19	8.00	1.40	0.48		1.99					3.87	0.04	0.06	0.32
16	7.80	0.20	8.00	1.13	0.87		1.83					3.83	0.14	0.23	0.03
17	7.66	0.34	8.00	1.52	0.15		2.65					4.32	0.04	0.04	
18	8.05	0.00	8.05	1.68	0.10		2.20					3.98	0.02		
19	7.85	0.15	8.00	1.15	0.38		2.53	0.08				4.14			
20	7.98	0.21	8.19	1.29	0.37		1.96		0.03			3.62	0.32		
21	7.89	0.11	8.00	1.87	0.16		1.91					3.94	0.05		0.03
22	7.64	0.36	8.00	1.73	0.63		1.45					3.81	0.08		
23	7.79	0.21	8.00	1.52	0.31		1.89	0.05				3.77	0.31	0.05	0.08
24	7.43	0.57	8.00	1.58	0.65		1.66					3.89	0.06	0.21	0.14
25	7.35	0.65	8.00	1.29	0.47		2.20					3.96	0.20	0.12	0.45
26	7.66	0.34	8.00	1.48	0.46		2.02	0.03				3.99	0.05	0.15	0.13
27	7.58	0.42	8.00	0.87	0.81		2.42	0.08				4.18	0.08	0.08	0.03
28	7.50	0.50	8.00	1.68	0.54		1.77					3.99		0.27	
29	7.79	0.21	8.00	1.06	0.56		2.46	0.02				4.10	0.06	0.06	0.03
30	7.70	0.30	8.00	1.27	0.63		2.06	0.06				4.02	0.06	0.06	0.05
31	7.86	0.14	8.00	2.11	0.22		1.12					3.45	0.43	0.00	0.00
32	7.64	0.36	8.00	2.27	0.23		1.40					3.90	0.02	0.00	0.00
33	7.61	0.39	8.00	1.81	0.00		2.52					4.33	0.04	0.00	0.00
34	7.33	0.67	8.00	2.37	0.00		1.69					4.06	0.08	0.00	0.00
35	7.99	0.01	8.00	1.62	0.05		1.90	0.05	0.45			3.62	0.00	0.08	0.00
36	8.04	0.00	8.04	1.05	0.08		2.75		0.00			3.88	0.08	0.00	0.00
37	7.52	0.48	8.00	2.08	0.17		1.37	0.04	0.00			3.66	0.15	0.30	0.16
38	7.60	0.40	8.00	1.22	0.39		1.75					3.36		0.17	
39	7.78	0.22	8.00	1.57	0.47		1.93					3.97		0.22	
40	7.71	0.29	8.00	1.79	0.62		1.32					3.73		0.46	
41	7.58	0.42	8.00	1.67	0.69		1.45					3.81		0.21	
42	7.85	0.15	8.00	1.86	0.20		1.81					3.87	0.07	0.10	
43	7.61	0.39	8.00	0.82	0.54		2.60	0.10				4.06	0.21	0.19	0.09
44	7.51	0.49	8.00	1.04	0.70		2.43					4.17	0.14	0.13	
45	7.93	0.07	8.00	1.34	0.28		2.48					4.10			
46	7.80	0.20	8.00	1.51	0.38		2.22					4.11		0.09	
47	7.82	0.18	8.00	1.57	0.20	0.03	2.04					3.84	0.36		
48	7.64	0.36	8.00	1.44	0.26		2.46					4.16	0.09	0.01	
49	7.81	0.19	8.00	1.65	0.40		1.88	0.02				3.95	0.04	0.13	
50	7.80	0.20	8.00	1.53	0.39		1.99	0.01				3.92	0.05	0.32	
51	7.62	0.38	8.00	1.58	0.39		1.61	0.05				3.63	0.11	0.18	
52	7.98	0.02	8.00	1.07	0.20		2.83	0.06				4.16	0.10	0.08	
53	7.81	0.19	8.00	1.33	0.30		2.42	0.04				4.09	0.17	0.08	
54	7.88	0.12	8.00	1.25	0.23		2.51	0.04				4.03	0.07	0.32	
55	7.87	0.13	8.00	1.46	0.40		2.12	0.02				4.00	0.03	0.14	
56	7.85	0.15	8.00	1.50	0.23		2.27	0.03				4.03	0.07	0.09	
57	7.82	0.18	8.00	1.53	0.44		1.98	0.01				3.96	0.01	0.03	
58	8.00		8.00	1.22	0.66		1.75	0.09				3.72		0.05	0.05
59	8.00		8.00	1.13	0.63		1.98	0.08				3.82	0.03	0.06	0.05
60	7.20	0.80	8.00	1.36	1.31		1.07	0.11		0.01		3.86		0.07	0.15
61	7.37	0.63	8.00	1.12	1.16		1.43	0.09		0.01		3.81	0.19	0.06	0.13
62	8.00		8.00	1.29	0.38		2.24	0.06				3.97		0.05	0.02

	Si	^{IV}Al	Στ	^{VI}Al	Fe(III)	Fe(II)	Mg	Ti	Fe(II)	Mn	Ca	Σo	Ca	K	Na
63	8.00		8.00	1.16	0.37		2.43	0.06				4.02	0.08	0.05	0.03
64	7.65	0.35	8.00	1.48	0.51		1.91	0.04		0.03		3.97	0.09	0.11	
65	7.70	0.30	8.00	1.73	0.53		1.54	0.02		0.03		3.85	0.07	0.17	
66	7.85	0.15	8.00	1.64	0.45		1.76	0.02		0.01		3.88	0.06	0.13	
67	7.64	0.36	8.00	1.35	0.58		2.04	0.05		0.02		4.04	0.08	0.11	
68	7.87	0.13	8.00	1.04	0.20		3.11					4.35	0.02	0.03	0.08
69	7.85	0.14	7.99	1.47	0.25		2.30					4.02	0.08	0.06	0.07
70	7.90	0.12	8.02	1.60	0.39		1.98					3.97	0.05	0.04	
71	7.91	0.09	8.00	1.48	0.37		2.25					4.10	0.01	0.02	
72	7.64	0.36	8.00	2.10	0.02		2.14					4.26	0.10	0.01	
73	7.84	0.16	8.00	2.00	0.06		1.96			0.04		4.06	0.03	0.04	0.02
74	7.82	0.18	8.00	1.33	0.04		3.00					4.37		0.02	0.22
75	7.68	0.32	8.00	0.89	0.68		2.78					4.35	0.86	0.04	0.10
76	7.94	0.06	8.00	0.68	0.07		3.91					4.66	0.16	0.02	
77	7.71	0.29	8.00	1.47	0.06		2.74					4.27	0.17		0.37
78	7.96	0.04	8.00	1.71	0.07		2.33					4.11	1.45	0.05	
79	7.77	0.23	8.00	1.50	0.33		1.90					3.73	0.47		0.19
80	8.02		8.02	0.92	0.49		2.70	0.06				4.17	0.03		
81	8.13		8.13	1.84	0.15		1.69					3.68	0.04	0.01	
82	8.02		8.02	0.92	0.49		2.70	0.06				4.17	0.03		
83	8.13		8.13	1.84	0.15		1.69					3.68	0.04	0.01	
84	7.81	0.19	8.00	1.66	0.36		1.83					3.85	0.01	0.45	
85	7.60	0.40	8.00	1.58	0.40		1.79					3.77	0.24	0.40	
86	7.85	0.15	8.00	1.72	0.07		2.10	0.03				3.92	0.23		
87	7.83	0.17	8.00	1.58	0.19	0.03	2.04					3.84	0.36		
88	7.82	0.18	8.00	2.02	0.09		1.97					4.08	0.01	0.01	
89	7.80	0.20	8.00	1.92	0.11		2.09					4.12	0.01		0.01
90	7.83	0.17	8.00	1.86	0.18		1.61					3.65		0.03	0.12
91	7.49	0.50	7.99	1.19	0.26		2.66					4.11	0.28	0.02	0.03
92	8.00		8.00	0.82	0.48		2.70	0.06				4.06			
93	8.00		8.00	1.68	0.23		2.12					4.03			
94	8.01		8.01	1.61	0.53		2.35					4.49	0.11	0.28	
95	7.95	0.05	8.00	1.49	0.61		1.73					3.83			
96	7.64	0.36	8.00	0.70	1.05		2.23	0.02				4.00	0.18	0.06	0.03
97	8.00		8.00	1.89	0.05		1.99	0.01				3.94	0.07		
98	7.79	0.21	8.00	1.64	0.42		1.90					3.96	0.03	0.12	
99	7.27	0.73	8.00	0.94	0.02		1.90				0.01	2.87			
100	7.27	0.73	8.00	0.94	0.02		1.90				0.01	2.87			
101	7.48	0.52	8.00	1.24	0.94		1.77	0.03				3.98			
102	7.64	0.36	8.00	1.44	0.26		2.46					4.16			
103	7.80	0.20	8.00	1.13	0.87		1.83					3.83	0.14	0.23	0.03
104	8.00		8.00	1.19	0.33		2.60					4.12	0.06	0.10	0.02
105	7.95	0.05	8.00	1.63	0.25		2.25					4.13		0.06	0.01
106	7.08	0.98	8.06	2.64	0.29	1.60	2.10					6.63	0.10		
107	8.02		8.02	1.91	0.04		2.01					3.96	0.01		0.07
108	7.85	0.15	8.00	1.57	0.24		2.21					4.02	0.03	0.11	
109	7.95	0.05	8.00	1.93	0.08		1.92					3.93	0.03	0.01	0.09
110	7.74	0.26	8.00	0.81	1.12		2.11					4.04	0.01	0.06	0.15
111	7.80	0.20	8.00	2.00	0.80		1.10					3.90		0.40	
112	7.43	0.58	8.01	1.49	0.83		1.54					3.86			
113	7.38	0.62	8.00	0.96	0.62		2.86					4.44			

1–11 compiled by Newman and Brown (1987); 12–14 from Galán and Carretero (1999); 15–45 compiled by Galán and Carretero (1999); 46–48 compiled by Jones and Galán (1991); 49–57 from Zaaboub *et al.* (2005); 58–63 from Torres-Ruiz *et al.* (1994); 64–67 from Jamoussi *et al.* (2003); 68–71 from García-Romero *et al.* (2004); 72–79 from Post and Crawford (2007); 80–81 from Neaman and Singer (2000); 82–83 from Weaver and Polland (1973); 84–85 from Weaver (1984); 86–87 from Imai and Otsuka (1984); 88–89 from Post and Heaney (2008); 90–91 from Corma *et al.* (1987); 92 from Singer and Norrish (1974); 93 from Güven (1992); 94 from Verrecchia and Le Coustumer (1996); 95 from López-Galindo (1987); 96 from Akbulut and Kadir (2003); 97 from Tien (1973); 98 from López-Galindo *et al.* (1996); 99 from Artioli *et al.* (1994); 100 from Artioli and Gali (1994); 101 from Li *et al.* (2007); 102 Galán *et al.* (1975); 103 from Siddiki (1984); 104 from Chahi *et al.* (2002); 105 from Giusteto *et al.* (2006); 106 from Suárez *et al.* (1994); 107 from Suárez and García-Romero (2006); 108 from Suárez *et al.* (2007); 109 from García-Romero *et al.* (2006); 110 from Gionis *et al.* (2006); 111 from Magalhaes *et al.* (2008); 112 from López-Galindo *et al.* (2008); and 113 from Chen *et al.* (2008).

cannot be ruled out completely. In the case when impurities were present, accurate comparison of chemical compositions was precluded. Prior to obtaining the mean structural formulae, a certain number of the analyses obtained was eliminated, using the following criteria. First, the formulae that did not have a good balance of charges were deleted, assuming instrumental errors in such cases. Also removed were all those analyses that had too many Si atoms or too many octahedral cations. Whether a formula for sepiolite with >12 atoms of Si or for palygorskite with >8 atoms of Si is the result of an instrumental error or because of adsorbed amorphous silica is unknown. In any case, excess silica which is too great cannot correspond to tetrahedral positions. Taking into account that sepiolite has 12 tetrahedral positions (p.h.u.c.) the formulae with $\geqslant 12.2$ Si atoms were removed. Samples may contain a small amount of amorphous silica which is impossible to avoid. Equally, sepiolite has eight octahedral positions and the analyses with >8 octahedral cations were eliminated. For the same reason, for palygorskites, analyses containing $\geqslant 8.2$ Si or $\geqslant 5$ octahedral positions occupied (p.h.u.c.) were removed. Remaining were 1223 definitive analytical data for the structural formulae calculations (454 from sepiolite and 779 from palygorskite). Approximately half of the data removed corre-

Table 4. Chemical composition (mean values, wt.% oxides) of the sepiolite samples studied.

		SiO_2	Al_2O_3	Fe_2O_3	MgO	TiO_2	CaO	NaO	K_2O	Σ
BAT	$N = 19$	67.48	4.31	2.13	23.41	1.12	0.94	0.12	0.56	100.07
	STDV	1.73	1.29	1.19	2.70	1.18	0.91	0.33	0.56	0.32
BOS	$N = 14$	66.70	2.75	2.14	25.33		1.54		1.34	99.80
	STDV	3.47	1.80	1.59	2.88		1.44		1.61	0.83
FIN	$N = 22$	66.46	2.82	3.22	25.60	0.04	1.08	0.17	0.63	100.01
	STDV	2.05	1.21	1.18	1.70	0.10	0.97	0.26	0.84	0.13
GRA	$N = 13$	69.01	0.49	0.44	29.19		0.34	0.43	0.10	100.00
	STDV	0.68	0.34	0.44	0.84		0.33	0.44	0.08	0.01
HEN	$N = 33$	68.54	0.83	0.59	29.27	0.01	0.31	0.21	0.19	99.95
	STDV	0.75	0.57	0.48	0.95	0.06	0.36	0.43	0.27	0.10
HUN	$N = 24$	66.09	5.24	2.61	23.13		0.78	0.94	1.19	99.97
	STDV	1.97	2.21	1.08	2.04		0.92	0.83	0.83	0.06
LIE	$N = 15$	69.43	5.97	2.44	21.38	0.01	0.31	0.39	0.04	99.89
	STDV	0.86	2.14	1.29	2.84	0.03	0.12	0.12	0.09	0.17
MAR	$N = 30$	67.57	3.40	2.04	26.22	0.13	0.24	0.04	0.27	100.03
	STDV	1.80	1.87	1.45	1.55	0.32	0.39	0.08	0.31	0.24
MER	$N = 6$	69.04	0.25	0.07	30.57		0.02		0.06	100.00
	STDV	0.44	0.27	0.11	0.33		0.04		0.09	0.01
MON	$N = 23$	68.59	1.43	1.61	27.72		0.34		0.18	99.95
	STDV	1.37	1.17	0.81	1.14		0.18		0.20	0.19
NAM	$N = 20$	68.74	1.18	0.70	28.78		0.55		0.16	100.11
	STDV	1.28	0.70	0.92	1.12		0.50		0.27	0.30
NEI	$N = 25$	66.77	2.20	1.88	27.48		0.87	0.01	0.76	99.96
	STDV	3.85	2.07	2.45	2.55		1.25	0.06	0.93	0.09
NEV	$N = 31$	66.52	2.35	1.53	28.01		0.88	0.11	0.59	99.99
	STDV	2.72	1.08	1.07	1.97		1.29	0.25	0.41	0.07
NOR	$N = 26$	68.49	1.12	0.38	28.78	0.15	0.34	0.19	0.46	99.91
	STDV	1.33	1.38	0.45	1.52	0.30	0.54	0.35	1.09	0.27
POL	$N = 22$	65.39	8.35	4.56	18.58	1.02	1.18		0.78	99.88
	STDV	0.40	2.09	2.34	4.06	0.88	0.53		0.40	0.18
SAN	$N = 12$	69.02	0.20	0.44	29.64		0.30	0.27	0.13	99.99
	STDV	0.56	0.20	0.29	0.75		0.21	0.41	0.18	0.03
SOM	$N = 22$	68.38	1.14	0.53	29.30		0.27	0.12	0.24	100.00
	STDV	1.28	0.74	0.59	0.75		0.38	0.20	0.38	0.07
TPO	$N = 11$	69.02	0.34	0.35	29.95		0.21	0.13		100.00
	SATDV	0.57	0.36	0.31	0.61		0.29	0.29		0.01
VAL	$N = 17$	68.01	2.01	0.64	28.20	0.31	0.29	0.12	0.34	99.80
	STDV	2.22	1.11	0.83	1.41	0.52	0.56	0.46	0.57	0.54
VIC	$N = 20$	67.25	2.37	1.79	27.72	0.02	0.50	0.04	0.27	99.97
	STDV	2.30	1.29	2.16	1.96	0.09	0.67	0.17	0.40	0.19
XIX	$N = 6$	69.67	0.05	0.89	29.08		0.11	0.20		100.00
	STDV	0.40	0.12	0.44	0.58		0.17	0.49		0.01
YUN	$N = 20$	69.50	1.04	0.30	28.78	0.00	0.15	0.10	0.05	100.00
	STDV	0.44	0.23	0.15	0.36	0.02	0.07	0.14	0.07	0.01

sponded to analyses with too much silica, probably adsorbed amorphous silica but possibly also related to instrumental errors.

The chemical compositions of the samples can be compared from mean values of oxide percentages (Tables 4, 5). Sepiolite has a mean SiO_2 content which ranges between 65.39% (POL and FIN samples) and 69.67% (XIX sample). The MgO content varies greatly between 30.57% in the most magnesic sample (MER) and 18.58% in the POL sample which, in accord with the Mg content, has the greatest proportion of Al_2O_3 (8.35%). Three samples have an Al_2O_3 content of <4%. Fe_2O_3 ranges between 3.22% and 0.07% (FIN and MER, respectively), although 70% of the samples have <2% of this oxide. The contents of other oxides such as TiO_2, K_2O, and Na_2O are generally small or zero. The mean contents are somewhat greater (~1% TiO_2 in BAT, BOS, and POL, or 0.94% Na_2O in HUN) but the standard deviation is similar to the mean value which indicates the variability of these oxides in the AEM analyses. CaO is present in all the sepiolites studied with variable content and a large standard deviation.

Palygorskite samples have SiO_2 contents which range between 72.93% (LIL sample) and 68.90% (BOA sample) and show a great variability in terms of the

Table 5. Chemical composition (mean values, wt.% oxides) of the palygorskite samples studied.

		SiO_2	Al_2O_3	Fe_2O_3	MgO	TiO_2	CaO	NaO	K_2O	Σ
ATT	$N = 8$	69.58	12.11	3.27	13.73	0.00	0.65	0.26	0.36	99.95
	STDV	0.76	0.98	0.53	0.99	0.01	0.30	0.37	0.24	0.07
BER	$N = 6$	70.04	12.97	4.54	11.76		0.43		0.25	100.00
	STDV	1.08	2.03	0.47	1.50		0.27		0.25	0.01
BOA	$N = 72$	68.90	13.88	4.16	11.28		0.36	0.95	0.64	100.15
	STDV	2.21	1.44	1.38	1.13		0.51	0.84	0.66	0.31
CAS	$N = 39$	71.38	14.46	1.76	10.75		0.48	0.62	0.54	100.02
	STDV	1.68	0.95	0.93	0.75		0.35	0.79	0.54	0.47
E 10	$N = 41$	70.42	7.52	1.64	19.82		0.25		0.28	99.92
	STDV	1.46	1.57	1.08	1.89		0.50		0.37	0.40
E 11	$N = 96$	69.44	10.04	2.05	17.33	0.01	0.38	0.47	0.31	100.03
	STDV	7.21	6.45	0.92	2.50	0.03	0.55	1.37	0.33	0.59
LIB	$N = 12$	71.88	12.31	1.74	13.37	0.33	0.11	0.21	0.02	99.99
	STDV	0.92	0.70	0.58	0.64	0.56	0.10	0.20	0.04	0.03
LIL	$N = 20$	72.93	14.56	0.29	11.75	0.01	0.17	0.36	0.02	100.10
	STDV	0.93	0.68	0.26	0.95	0.03	0.20	0.64	0.03	0.36
MET	$N = 12$	72.16	13.51	0.57	13.04		0.64		0.10	100.00
	STDV	0.86	0.95	0.81	1.05		0.61		0.24	0.01
NIJ	$N = 13$	71.71	12.61	2.12	12.57	0.06	0.09	0.85	0.03	100.05
	STDV	1.00	3.42	1.65	1.67	0.19	0.06	0.43	0.04	0.18
OKE	$N = 48$	71.26	15.88	0.38	11.38	0.01	0.15	0.63	0.11	99.80
	STDV	1.23	0.65	0.43	1.01	0.02	0.26	0.56	0.26	0.42
PAL	$N = 63$	71.41	15.03	0.22	12.37	0.00	0.37	0.45	0.15	100.00
	STDV	1.71	1.37	0.34	1.70	0.02	0.43	0.54	0.31	0.01
PIC	$N = 52$	70.08	9.99	5.54	13.21	0.14	0.18	0.74	0.07	99.96
	STDV	0.88	0.71	0.51	0.66	0.33	0.19	0.49	0.11	0.15
SEG	$N = 46$	71.07	15.84	0.68	11.16	0.01	0.41	0.74	0.08	99.99
	STDV	1.56	1.06	0.51	0.96	0.05	0.65	0.65	0.14	0.25
TOR	$N = 17$	70.08	11.59	4.48	13.60		0.06		0.08	99.90
	STDV	0.61	0.83	0.59	0.92		0.11		0.14	0.13
TRA	$N = 20$	71.42	9.21	1.83	16.91	0.09	0.38		0.13	99.97
	STDV	1.00	0.72	0.36	1.05	0.52	0.40		0.17	0.13
Y0	$N = 28$	70.25	12.17	4.01	12.49	0.06	0.19	0.37	0.43	99.97
	STDV	1.90	1.82	1.81	1.25	0.12	0.20	0.65	0.62	0.07
Y1A	$N = 30$	71.49	11.83	1.96	14.30		0.26	0.09	0.08	100.01
	STDV	1.01	1.78	0.89	1.63		0.37	0.29	0.17	0.03
Y3	$N = 14$	71.72	11.92	1.60	14.08	0.07	0.12	0.18	0.31	10.00
	STDV	1.03	0.95	0.43	0.96	0.10	0.15	0.27	0.30	0.01
Y7	$N = 15$	71.26	12.75	2.08	13.27	0.05	0.21	0.31	0.08	98.16
	STDV	1.41	1.04	0.96	0.87	0.18	0.31	0.53	0.18	4.45
Y8	$N = 15$	70.60	13.46	2.43	12.91	0.07	0.06	0.05	0.42	10.00
	STDV	1.06	1.23	0.43	0.78	0.14	0.09	0.09	0.28	0.01
YUC	$N = 11$	71.45	11.36	3.02	14.01		0.07	0.06	0.03	100.00
	STDV	1.47	1.16	1.52	1.17		0.24	0.19	0.08	0.01

contents of the oxides of the main octahedral cations. Al_2O_3 ranges between 15.88 and 7.52% (OKE and E10, respectively) and MgO between 19.82 and 10.75% (E10 and CAS, respectively). All of the samples studied contain Fe_2O_3 with the amount reaching 5.54% in the PIC sample, with standard deviation equal to 0.51, which indicates that in general all analyses corresponding to this sample contain a large amount of Fe. TiO_2 is absent from nine samples and in the rest the content is very small. Na_2O, K_2O, and CaO appear as minor components, CaO occurring in all samples studied. Both minerals present a great variability in terms of amounts of the main oxides (Tables 4, 5). In fact, if the amounts of oxides of the main octahedral cations are plotted (Figure 1), the analyses appear to be projected in a continuous region without separation between the two minerals.

The mean values of each cation, the total, tetrahedral, and octahedral contents (p.h.u.c), and the standard deviation for all are shown together with Si/Mg and R3/R2 relations (Tables 6, 7). The number of Si atoms ranges from 11.50 to 12.11 for sepiolite and from 7.88 to 8.06 for palygorskite. The number of total octahedral cations ranges from 6.87 to 7.95 for sepiolite and from 3.35 to 4.40 for palygorskite. These values correspond to 0.6–14% octahedral vacancies for sepiolite and between 12 and 23.6% for palygorskite. Clearly, Mg is the main octahedral cation in sepiolite (4.88–7.92) and this mineral contains only minor amounts of Al (0.01–1.24) and Fe(III) (0.01–0.43). Palygorskite shows greater octahedral variability: Mg (1.79–3.34), Al (0.92–1.99), and Fe(III) (0.02–0.47). Most of the analyses of each sample range between narrow limits, as indicated by the small values for standard deviation

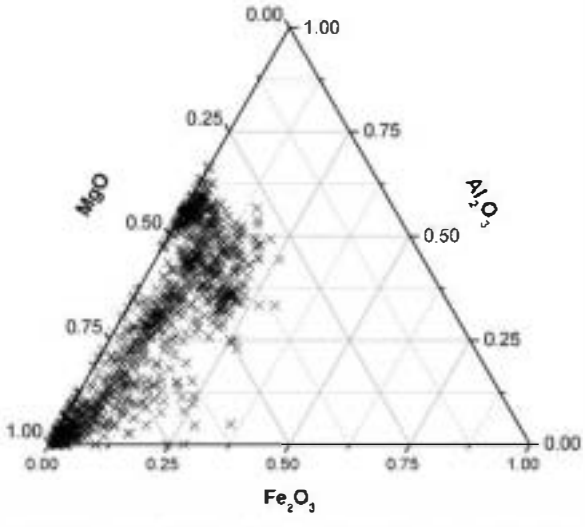

Figure 1. AFM diagram for the sepiolites and palygorskites studied. All points analyzed are projected between the two extremes, but with no separation between data corresponding to sepiolites and palygorskites.

(Tables 6, 7). Very small amounts of Ti appear in the mean structural formulae of several sepiolites. Ca is always present as an exchangeable cation and Na and K are present in most samples.

DISCUSSION

Due to the large number of samples studied in the present work, several chemical variations were found. The structural formulae proposed for the samples studied (Tables 8, 9) are from the mean values of each cation obtained (Tables 6, 7). Regarding the tetrahedral composition, theoretical sepiolite has twelve tetrahedral positions and palygorskite eight, although a few of these positions can be partially filled by Al and sepiolite could have Fe in tetrahedral positions. A certain number of samples of sepiolite have Fe(III) as a tetrahedral cation (Table 6), in very small amounts (<0.04) and with standard deviation even greater than the mean. Regarding the octahedral content, the natural palygorskites show a wider range of substitutions than sepiolites, which can correspond to different types. The MER, TPO, and SAN sepiolites have a structural formula close to the theoretical, both for the tetrahedral and the octahedral content. The MER sample is the most 'perfect' sepiolite from these data, in good agreement with those published by Ece (1998) for sepiolite from the same locality. Twelve samples contain variable amounts of tetrahedral Al, with >7 atoms of Mg p.h.u.c. (between 90 and 95% of the octahedral positions occupied by Mg) and minor amounts of Al and Fe(III); the remainder of the samples (MAR, BOS, FIN, BAT, HUN, and POL) are characterized by the greater octahedral substitution and these six samples also present tetrahedral substitution. These most Al-rich and/or Fe-rich sepiolites have between 61 and 85% of the octahedral positions occupied by Mg.

When comparing these results with those which appear in the literature (Table 2), some sepiolites show the same characteristics: smaller Mg content than the ideal composition, due to substitution by Al and/or Fe(III). This seems to indicate that Al-rich sepiolite is not so rare. The Mg content *vs.* total octahedral content was plotted (Figure 2), both for data from the literature and for those from the present study. The same distribution for the two types of data was found. As expected, most of the points plotted in the region with the greatest Mg values with the largest number of octahedral cations because sepiolite may not have octahedral substitution (Galán and Carretero, 1999). A certain number of analyses correspond to the most dioctahedral extremes and the smallest Mg contents and equate to Al-rich sepiolites such as that referred to by Rogers *et al.* (1956). Imai and Otsuka (1984) reported Fe-rich palygorskite, and García-Romero *et al.* (2007) reported very Al-rich sepiolite together with a very Mg-rich palygorskite in the Allou Kagne deposit (Senegal). Looking at the data both from the literature and from

Table 6. Mean values of tetrahedral and octahedral cations, and Si/Mg and R3/R2 relations for the sepiolite samples, calculated from the structural formulae.

		Si	^{IV}Al	Fe^{3+}	Στ	^{VI}Al	Fe^{3+}	Mg	Ti	Σo	Ca	K	Na	Si/Mg	R3/R2
BAT	*N* = 19	11.81	0.21		12.02	0.68	0.28	6.10	0.13	7.2	0.18	0.12	0.04	1.94	0.16
	STDV	0.22	0.2		0.04	0.29	0.16	0.69	0.12	0.36	0.17	0.13	0.11		
BOS	*N* = 14	11.77	0.27	0	12.04	0.31	0.28	6.71		7.31	0.29	0.31		1.75	0.09
	STDV	0.4	0.36	0.01	0.06	0.17	0.21	0.59		0.37	0.28	0.38			
FIN	*N* = 14	11.72	0.3	0	12.01	0.29	0.43	6.72	0.01	7.45	0.21	0.15	0.06	1.74	0.11
	STDV	0.27	0.25	0.01	0.04	0.16	0.16	0.45	0.01	0.26	0.18	0.2	0.09		
GRA	*N* = 13	12.02	0.02		12.04	0.09	0.05	7.58		7.71	0.07	0.02	0.15	1.59	0.02
	STDV	0.09	0.03		0.06	0.07	0.06	0.22		0.16	0.06	0.02	0.15		
HEN	*N* = 33	11.95	0.05	0.01	12.01	0.11	0.07	7.61	0.00	7.79	0.06	0.04	0.07	1.57	0.02
	STDV	0.10	0.07	0.02	0.04	0.12	0.06	0.25	0.01	0.15	0.07	0.06	0.15		
HUN	*N* = 24	11.66	0.34		12.00	0.75	0.35	6.08		7.18	0.15	0.27	0.32	1.92	0.18
	STDV	0.29	0.29		0.00	0.33	0.15	0.53		0.27	0.17	0.19	0.28		
LIE	*N* = 15	12.02	0.04		12.06	1.18	0.32	5.52		7.02	0.06	0.04	0.13	2.18	0.27
	STDV	0.14	0.10		0.05	0.40	0.18	0.74		0.30	0.02	0.11	0.04		
MAR	*N* = 30	11.80	0.25		12.04	0.45	0.28	6.82	0.02	7.57	0.05	0.06	0.01	1.73	0.11
	STDV	0.29	0.24		0.06	0.21	0.18	0.40	0.04	0.22	0.07	0.07	0.03		
MER	*N* = 6	11.99	0.02		12.01	0.03	0.01	7.92		7.95	0.01	0.01		1.51	0.01
	STDV	0.06	0.04		0.03	0.04	0.01	0.10		0.06	0.01	0.02			
MON	*N* = 23	11.97	0.08	0.00	12.05	0.22	0.21	7.21		7.66	0.07	0.04		1.66	0.06
	STDV	0.19	0.14	0.01	0.06	0.16	0.10	0.30		0.16	0.04	0.05			
NAM	*N* = 20	11.97	0.09		12.06	0.16	0.08	7.45		7.69	0.10	0.04		1.61	0.03
	STDV	0.16	0.09		0.10	0.10	0.12	0.35		0.23	0.10	0.06			
NEI	*N* = 25	11.73	0.25	0.04	12.02	0.21	0.21	7.20		7.62	0.18	0.16	0.01	1.63	0.06
	STDV	0.47	0.36	0.13	0.06	0.22	0.25	0.58		0.27	0.25	0.21	0.03		
NEV	*N* = 31	11.68	0.30	0.01	11.99	0.17	0.19	7.40		7.73	0.16	0.12	0.04	1.58	0.05
	STDV	0.35	0.29	0.05	0.09	0.15	0.04	0.36		0.20	0.24	0.10	0.09		
NOR	*N* = 26	11.95	0.09		12.04	0.14	0.05	7.48	0.01	7.69	0.06	0.10	0.06	1.60	0.03
	STDV	0.15	0.11		0.07	0.22	0.06	0.37	0.04	0.20	0.10	0.25	0.12		
POL	*N* = 22	11.50	0.50		12.00	1.24	0.61	4.88	0.14	6.87	0.22	0.19		2.36	0.38
	STDV	0.04	0.03		0.01	0.42	0.31	1.04	0.12	0.38	0.10	0.09			
SAN	*N* = 12	12.02	0.02	0.00	12.04	0.02	0.06	7.69		7.77	0.06	0.01	0.09	1.56	0.01
	STDV	0.08	0.04	0.01	0.05	0.03	0.04	0.19		0.16	0.03	0.02	0.14		
SOM	*N* = 22	11.92	0.11		12.03	0.13	0.07	7.61		7.81	0.05	0.06	0.03	1.57	0.03
	STDV	0.17	0.15		0.05	0.09	0.08	0.18		0.12	0.07	0.09	0.06		
TPO	*N* = 11	12.00	0.03		12.03	0.04	0.05	7.76		7.85	0.04		0.04	1.55	0.01
	SATDV	0.08	0.04		0.05	0.06	0.04	0.17		0.13	0.05		0.10		
VAL	*N* = 17	11.86	0.17	0.01	12.04	0.25	0.06	7.35	0.03	7.69	0.05	0.08	0.06	1.61	0.04
	STDV	0.29	0.23	0.04	0.05	0.15	0.10	0.36	0.06	0.20	0.11	0.13	0.18		
VIC	*N* = 20	11.77	0.23	0.01	12.01	0.27	0.23	7.22	0.00	7.73	0.10	0.06	0.01	1.63	0.07
	STDV	0.29	0.27	0.03	0.02	0.18	0.29	0.46	0.01	0.17	0.13	0.08	0.06		
XIX	*N* = 6	12.11			12.11	0.01	0.12	7.53		7.53	0.02		0.07	1.61	0.02
	STDV	0.06			0.06	0.02	0.06	0.14		0.14	0.03		0.16		
YUN	*N* = 20	12.06			12.07	0.21	0.03	7.45		7.69	0.02	0.01	0.03	1.62	0.03
	STDV	0.05			0.04	0.05	0.02	0.09		0.08	0.01	0.01	0.05		

AEM in this study, sepiolite can be classified into two groups: sepiolite and Al-sepiolite. A limit for these two groups can be established from the octahedral occupancy and Al-sepiolites are those that have >10% of octahedral positions vacant and >0.5 ^{VI}Al atoms (Table 6).

Palygorskite has greater compositional variation than sepiolite. The ideal palygorskite has filled four of its five octahedral positions (2 Mg and 2 Al). According to Suárez *et al.* (2007), based on the octahedral composition, palygorskite could be of three different types: (1) Ideal palygorskite, with an octahedral composition near to the ideal palygorskite, similar contents of Al and Mg, and negligible substitutions. (2) Common palygorskite, where the ^{VI}Al content is less than in the ideal formula and as a consequence the Mg content is greater, but the number of octahedral cations is close to 4 (vacant octahedral positions = 1). Although Al may be partially substituted by Fe(III) and/or Mg, this type of palygorskite has dioctahedral character. (3) Magnesic palygorskite is the most trioctahedral extreme. The number of octahedral cations is >4 (vacant octahedral positions 1). Palygorskite can, on occasion, be Fe-rich, such as the

Table 7. Mean values of tetrahedral and octahedral cations, Si/Mg and R3/R2 relations for the samples of palygorskite calculated from the structural formulae.

		Si	^{IV}Al	Στ	^{VI}Al	Fe^{3+}	Mg	Ti	Σo	Ca	K	Na	Si/Mg	R3/R2
ATT	*N* = 8	7.86	0.14	8.00	1.47	0.28	2.31	0.00	4.06	0.08	0.05	0.06	3.40	0.76
	STDV	0.07	0.07	0.01	0.08	0.04	0.16	0.01	0.07	0.04	0.03	0.08		
BER	*N* = 6	7.90	0.12	8.02	1.60	0.39	1.98		3.97	0.05	0.04		3.99	1.01
	STDV	0.12	0.09	0.04	0.20	0.04	0.25		0.11	0.03	0.04			
BOA	*N* = 72	7.80	0.21	8.00	1.64	0.35	1.91		3.91	0.04	0.09	0.21	4.08	1.04
	STDV	0.17	0.17	0.02	0.17	0.12	0.19		0.11	0.06	0.10	0.19		
CAS	*N* = 39	7.98	0.06	8.04	1.88	0.15	1.79		3.81	0.06	0.08	0.12	4.46	1.13
	STDV	0.13	0.09	0.06	0.11	0.08	0.12		0.11	0.04	0.08	0.18		
E 10	*N* = 41	7.95	0.08	8.03	0.92	0.14	3.34		4.40	0.03	0.04		2.38	0.32
	STDV	0.13	0.10	0.05	0.19	0.09	0.32		0.16	0.06	0.05			
E 11	*N* = 96	7.92	0.10	8.02	1.14	0.18	2.92	0.00	4.25	0.04	0.04	0.06	2.71	0.45
	STDV	0.15	0.13	0.04	0.20	0.08	0.41	0.01	0.21	0.05	0.05	0.11		
LIB	*N* = 12	7.98	0.03	8.01	1.61	0.16	2.27	0.01	4.05	0.02		0.05	3.53	0.78
	STDV	0.09	0.05	0.06	0.07	0.02	0.11	0.01	1.57	0.01		0.04		
LIL	*N* = 20	8.06	0.03	8.10	1.89	0.02	1.95		3.85	0.01		0.07	4.13	0.98
	STDV	0.07	0.13	0.14	0.08	0.02	0.17		0.12	0.02		0.13		
MET	*N* = 12	8.02	0.02	8.04	1.75	0.05	2.16		3.95	0.08	0.01		3.71	0.83
	STDV	0.08	0.04	0.05	0.11	0.07	0.17		0.13	0.07	0.02			
NIJ	*N* = 13	8.02	0.04	8.06	1.62	0.18	2.10		3.90	0.01	0.00	0.19	3.82	0.86
	STDV	0.11	0.06	0.07	0.40	0.14	0.30		0.13	0.01	0.01	0.10		
OKE	*N* = 48	7.92	0.09	8.01	1.99	0.03	1.88		3.91	0.02	0.02	0.14	4.21	1.07
	STDV	0.10	0.08	0.02	0.09	0.04	0.17		0.11	0.03	0.04	0.12		
PAL	*N* = 63	7.93	0.08	8.02	1.89	0.02	2.05		3.95	0.04	0.02	0.10	3.87	0.93
	STDV	0.15	0.13	0.05	0.20	0.03	0.30	0.00	0.16	0.05	0.04	0.12		
PIC	*N* =52	7.96	0.05	8.01	1.28	0.47	2.24	0.01	4.01	0.02	0.01	0.16	3.55	0.78
	STDV	0.08	0.06	0.03	0.08	0.04	0.11	0.03	0.07	0.02	0.02	0.11		
SEG	*N* = 46	7.90	0.11	8.02	1.97	0.06	1.85		3.88	0.05	0.01	0.16	4.27	1.10
	STDV	0.14	0.12	0.04	0.11	0.04	0.17		0.11	0.08	0.02	0.14		
TOR	*N* = 17	7.88	0.12	8.00	1.43	0.38	2.28		4.09	0.01	0.02		3.46	0.79
	STDV	0.08	0.07	0.01	0.10	0.05	0.16		0.06	0.01	0.03			
TRA	*N* = 20	8.02	0.02	8.03	1.20	0.15	2.83	0.01	4.19	0.05	0.02		2.83	0.48
	STDV	0.08	0.08	0.05	0.11	0.03	0.18	0.05	0.12	0.05	0.03			
YO	*N* = 28	7.93	0.11	8.04	1.51	0.34	2.10	0.01	3.96	0.02	0.06	0.08	3.78	0.88
	STDV	0.17	0.13	0.05	0.18	0.16	0.21	0.01	0.15	0.02	0.09	0.14		
Y1A	*N* = 30	7.99	0.04	8.03	1.52	0.16	2.38		4.07	0.03	0.01	0.02	3.36	0.71
	STDV	0.09	0.06	0.05	0.20	0.07	0.28		0.11	0.04	0.02	0.06		
Y3	*N* = 14	8.02	0.03	8.04	1.54	0.13	2.35	0.01	4.03	0.01	0.04	0.04	3.41	0.71
	STDV	0.09	0.04	0.06	0.11	0.04	0.16	0.01	0.10	0.02	0.04	0.06		
Y7	*N* = 15	7.96	0.07	8.03	1.62	0.17	2.21	0.00	4.01	0.03	0.01	0.07	3.60	0.81
	STDV	0.12	0.09	0.05	0.13	0.09	0.15	0.02	0.14	0.04	0.03	0.11		
Y8	*N* = 15	7.91	0.09	8.00	1.68	0.20	2.16	0.01	4.05	0.01	0.07	0.01	3.66	0.87
	STDV	0.11	0.10	0.02	0.08	0.04	0.13	0.01	0.07	0.01	0.04	0.02		
YUC	*N* = 11	8.00	0.03	8.04	1.47	0.23	2.34		4.04	0.04	0.00	0.01	3.42	0.73
	STDV	0.11	0.08	0.05	0.17	0.15	0.21		0.13	0.10	0.01	0.04		

Table 8. Structural formulae proposed for the sepiolites studied.

	Si	^{IV}Al	Στ	^{VI}Al	Fe^{3+}	Mg	Ti	Σo	Ca	K	Na
BAT	11.81	0.19	12.00	0.68	0.28	6.10	0.13	7.19	0.18	0.12	0.04
BOS	11.77	0.23	12.00	0.31	0.28	6.71		7.30	0.29	0.31	
FIN	11.72	0.28	12.00	0.12	0.61	6.66		7.46	0.25	0.17	0.05
GRA	12.00		12.00	0.09	0.05	7.58		7.72	0.07	0.02	0.15
HEN	11.95	0.05	12.00	0.11	0.07	7.61		7.79	0.06	0.04	0.07
HUN	11.66	0.34	12.00	0.75	0.35	6.08		7.18	0.15	0.27	0.32
LIE	12.00		12.00	1.18	0.32	5.52		7.02	0.06	0.04	0.13
MAR	11.80	0.20	12.00	0.45	0.28	6.82	0.02	7.57	0.05	0.06	0.01
MER	11.99	0.01	12.00	0.03	0.01	7.92		7.96	0.01	0.01	
MON	11.97	0.03	12.00	0.22	0.21	7.21		7.64	0.07	0.04	
NAM	11.97	0.03	12.00	0.16	0.08	7.45		7.69	0.10	0.04	
NEI	11.73	0.22	11.95	0.22	0.21	7.20		7.62	0.18	0.16	0.01
NEV	11.68	0.32	12.00	0.17	0.19	7.40		7.76	0.16	0.12	0.04
NOR	11.95	0.05	12.00	0.14	0.05	7.48	0.01	7.68	0.06	0.10	0.06
POL	11.50	0.50	12.00	1.24	0.61	4.88	0.14	6.87	0.22	0.19	
SAN	12.00		12.00	0.02	0.06	7.69		7.77	0.06	0.01	0.09
SOM	11.92	0.08	12.00	0.13	0.07	7.61		7.81	0.05	0.06	0.03
TPO	12.00		12.00	0.04	0.05	7.76		7.85	0.04		0.04
VAL	11.84	0.16	12.00	0.25	0.06	7.35	0.03	7.69	0.05	0.08	0.06
VIC	11.77	0.23	12.00	0.27	0.23	7.22		7.72	0.10	0.06	0.01
XIX	12.00		12.00	0.10	0.12	7.53		7.66	0.02		0.07
YUN	12.00		12.00	0.27	0.03	7.45		7.69	0.02	0.01	0.03
MAX	12.00	0.50		1.24	0.61	7.92	0.14	7.96	0.29	0.31	0.32
MIN	11.50	0.00		0.01	0.00	4.88	0.00	6.87	0.01	0.00	0.00
MEAN	11.87	0.13		0.32	0.19	7.06	0.02	7.57	0.10	0.09	0.06

Table 9. Structural formulae proposed for the palygorskites studied.

	Si	^{IV}Al	Στ	^{VI}Al	Fe^{3+}	Mg	Ti	Σo	Ca	K	Na
ATT	7.86	0.14	8.00	1.47	0.28	2.31		4.06	0.08	0.05	0.06
BER	7.90	0.10	8.00	1.60	0.39	1.98		3.97	0.05	0.04	
BOA	7.80	0.20	8.00	1.64	0.35	1.91		3.90	0.04	0.09	0.21
CAS	7.98	0.02	8.00	1.88	0.15	1.79		3.82	0.06	0.08	0.12
E10	7.95	0.05	8.00	0.92	0.14	3.34		4.40	0.03	0.04	
E11	7.92	0.08	8.00	1.14	0.18	2.92		4.24	0.04	0.04	0.06
LIB	8.00		8.00	1.61	0.16	2.27	0.01	4.05	0.02		0.05
LIL	8.00		8.00	1.89	0.02	1.95		3.86	0.01		0.07
MET	8.00		8.00	1.75	0.05	2.16		3.96	0.08	0.01	
NIJ	8.00		8.00	1.62	0.18	2.10		3.90	0.01		0.19
OKE	7.92	0.08	8.00	1.99	0.03	1.88		3.90	0.02	0.02	0.14
PAL	7.93	0.07	8.00	1.89	0.02	2.05		3.96	0.04	0.02	0.10
PIC	7.96	0.04	8.00	1.28	0.47	2.24	0.01	4.00	0.02	0.01	0.16
SEG	7.90	0.10	8.00	1.97	0.06	1.85		3.88	0.05	0.01	0.16
TOR	7.88	0.12	8.00	1.43	0.38	2.28		4.09	0.01	0.02	
TRA	8.00		8.00	1.20	0.15	2.83		4.19	0.05	0.02	
Y0	7.93	0.07	8.00	1.51	0.34	2.10	0.01	3.96	0.02	0.06	0.08
Y1A	7.99	0.01	8.00	1.52	0.16	2.38		4.06	0.03	0.01	0.02
Y3	8.00		8.00	1.54	0.13	2.35	0.01	4.03	0.01	0.04	0.04
Y7	7.96	0.04	8.00	1.62	0.17	2.21		4.00	0.03	0.01	0.07
Y8	7.91	0.09	8.00	1.68	0.20	2.16	0.01	4.05	0.01	0.07	0.01
YUC	8.00		8.00	1.47	0.23	2.34		4.04	0.04		0.01
MAX	8.00	0.20		1.99	0.47	3.34	0.01	4.40	0.08	0.09	0.21
MIN	7.86	0.00		0.92	0.02	1.79	0.00	3.82	0.01	0.00	0.00
MEAN	7.95	0.06		1.57	0.19	2.24	0.00	4.01	0.03	0.03	0.07

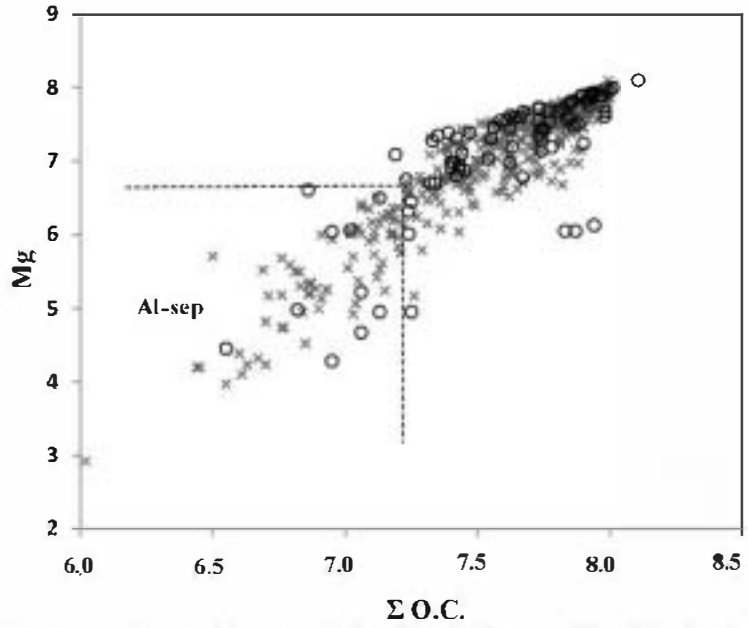

Figure 2. Mg content (p.h.u.c.) *vs.* total octahedral content, for data from the literature (●) and for data from the present study (×). The two kinds of data are projected in the same region of the plot.

Greek samples studied by Gionis *et al.* (2007). According to this classification most palygorskites studied here correspond to Type II and magnesic palygorskites (Type III) are E10, E11, and TRA. Among these, the smallest Al content corresponds to E10 (0.92), the most trioctahedral palygorskite found in the present study.

All structural formulae calculated from AEM analysis of palygorskite studied here and in the literature are projected taking into account the number of Mg (p.h.u.c.) *vs.* the octahedral content (total number of octahedral cations p.h.u.c.). When the samples studied here are compared to those in the literature, similar tendencies are found (Figure 3) and the data from the literature can also be classified into the types described previously.

With the literature data and new data coming from a very wide range of samples of different origins, however, a new type of palygorskite must be defined, namely the Type IV, 'aluminic palygorskite', the most

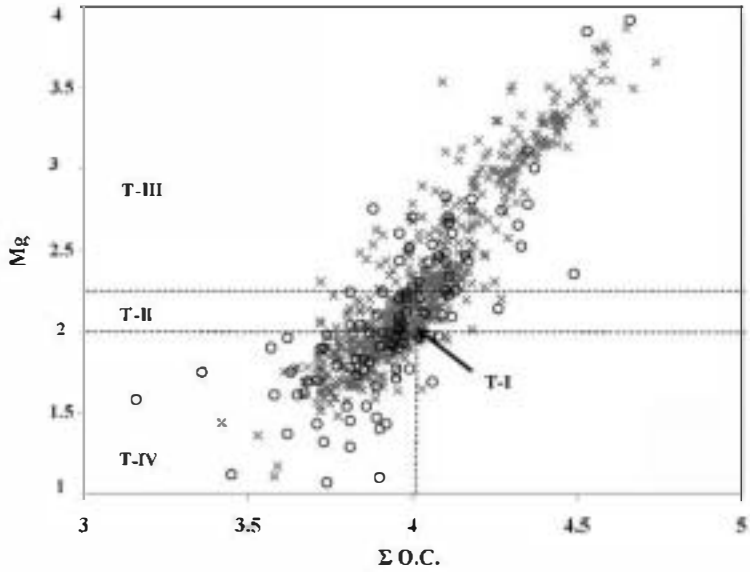

Figure 3. Number of Mg cations (p.h.u.c.) *vs* the total number of octahedral cations p.h.u.c. for palygorskites, for data from the literature (●) and for data from the present study (×). The diagram shows the four classifications (I–IV) described in the text.

dioctahedral extreme, which contains palygorskites with a total number of octahedral cations (p.h.u.c.) of <4, with R3/R2>1 and Mg<2. Taking into account the structural formulae proposed (Table 9) for the palygorskites from the present study, samples CAS, OKE, and SEG correspond to Type IV.

A category of Fe-rich palygorskite could be used when Fe>Al in the different types described above. Palygorskite studied by Gionis *et al.* (2006) is an Fe-rich palygorskite, Type II; and Chryssikos *et al.* (2009) studied several palygorskites rich in Fe, that could be classified as Fe-rich, Types I, II, and III. In the samples studied here, the Fe content can be large (≤ 0.47) but none could be referred to as Fe-rich. This classification of palygorskites could be formulated with the variables proposed by Gionis *et al.* (2007): *i.e.* where x, y refers to the palygorskite formula $y Mg_5Si_8O_{20}(OH)_2 \cdot (1-y)[xMg_2Fe_2(1-x)\ Mg_2Al_2]Si_8O_{20}(OH)_2$. Taking into account that y is an indication of the trioctahedral degree in palygorskite, y is negative in Type IV, ~0 in Type I, ranges between 0.1 and 0.2 in Type II, and >0.2 in Type III (the most trioctahedral option). In the same formula, x is an indication of the Fe content for all types of Fe-rich palygorskites where $x \geq 0.5$.

A great variability in the structural formula of the two minerals exists, especially in palygorskite. Several isomorphic substitutions are possible and this means that the occupancy of octahedral positions also varies. In both minerals, Al, Fe, and Mg can exist with very variable proportions. Martin-Vivaldi and Cano-Ruiz (1956) said, "the minerals of the palygorskite-sepiolite group occupy the region of discontinuity between dioctahedral and trioctahedral minerals," and comparing the samples in terms of octahedral occupancy is very useful. To compare the two minerals from their structural data the relation between Si/Mg cations and the occupancy of the octahedral position (in percentage) was used (Figure 4). The results corresponding to the structural formulae proposed for the samples studied in the present work are projected in the same graph as data taken from the literature. In the latter, greater dispersion was found due to the variety of methods of analyses and probably to the presence of impurities, but all samples are projected onto one curve. Three groups emerged: a group of samples of palygorskite which have the largest Si/Mg ratio and octahedral vacancies, a group of sepiolite samples with smaller values of these two variables, and a third group of samples in which both sepiolites and palygorskites are plotted. Mg-palygorskites and Al-sepiolites are plotted between the ordinary palygorskite and sepiolite groups.

The compositional limit between the two minerals was found by studying the oxides content and taking into account the fact that the samples studied here represent the general tendency found in the literature for these fibrous clay minerals (Figure 4).The mean SiO_2 content of the sepiolites and palygorskites is similar, as can be seen when comparing the mean values of major oxides contents obtained for the samples studied with the theoretical formulae of both minerals. The SiO_2 content is slightly smaller in sepiolite than in palygorskite and smaller than the ideal content for each mineral in general, as expected, taking into account that in all analyses, oxides other than SiO_2, Al_2O_3, and MgO have

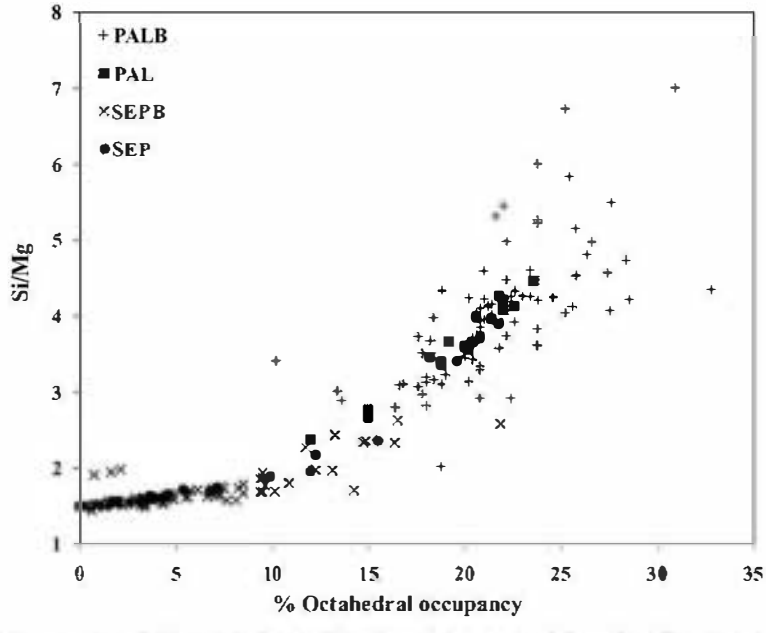

Figure 4. Comparison between the sepiolites and palygorskites from their structural formulae. The relation between Si/Mg and the octahedral occupancy (%) shows the same tendency both for data from the literature and for the data obtained in the present study and sepiolite and palygorskite are projected in a continuous region.

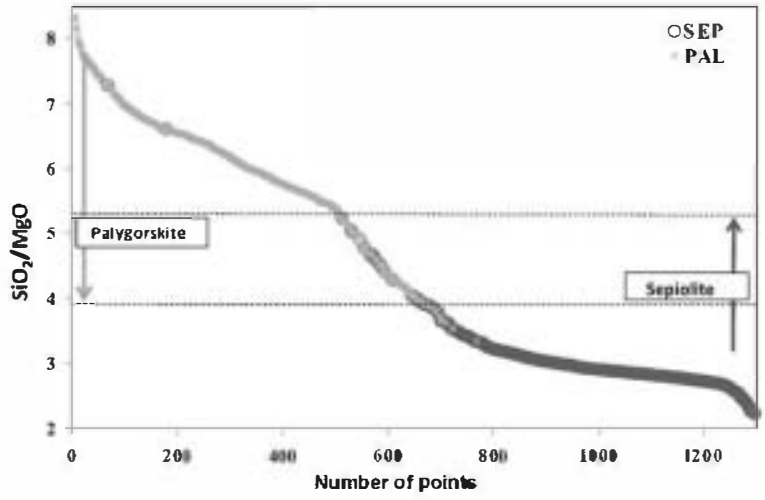

Figure 5. SiO_2/MgO ratios for all AEM analyses, ordered from the largest to the smallest values.

been detected. Only three sepiolites (XIX, YUN, and LIE) and one palygorskite (LIL) have a little more silica than these ideal compositions, indicating that these samples may contain adsorbed silica, especially sample XIX, in agreement with the structural formulae obtained.

The best way to compare the chemical composition is to compare the contents of the main oxides. When all of the particles analysed are plotted from the greatest to the smallest values of the relation between SiO_2 and MgO, a continuous curve is obtained (Figure 5) and no break in the data between palygorskites and sepiolites was found. On the contrary, both minerals overlap and a continuous compositional variation exists from the ideal sepiolite to the most Al-rich palygorskite (points with the largest SiO_2/MgO values). Each type of mineral (sepiolite and palygorskite) is projected into different domains. Logically, sepiolite plots in positions nearest to the smallest SiO_2/MgO values. Palygorskite can have SiO_2/MgO values of between ~7.5 and 3.0 and sepiolite from ~1.5 to 4.5, but in the range 3.0–4.5 both minerals are possible.

The same kind of plot (Figure 6) and conclusions are obtained if the amounts of different oxides of octahedral cations are considered ($Al_2O_3+Fe_2O_3/MgO$). Again, each type of mineral (sepiolite and palygorskite) is projected into a different domain, but the two domains overlap. Sepiolite, logically, is projected into the positions nearest to the smallest $(Al_2O_3+Fe_2O_3)/MgO$ values. Palygorskite can have $(Al_2O_3+Fe_2O_3)/MgO$ between ~0.25 and 2.2 and sepiolite from 0.0 to ~1.0, but in the range between 0.25–1 both minerals are possible.

Several samples, therefore, have intermediate chemical composition between the most extreme members,

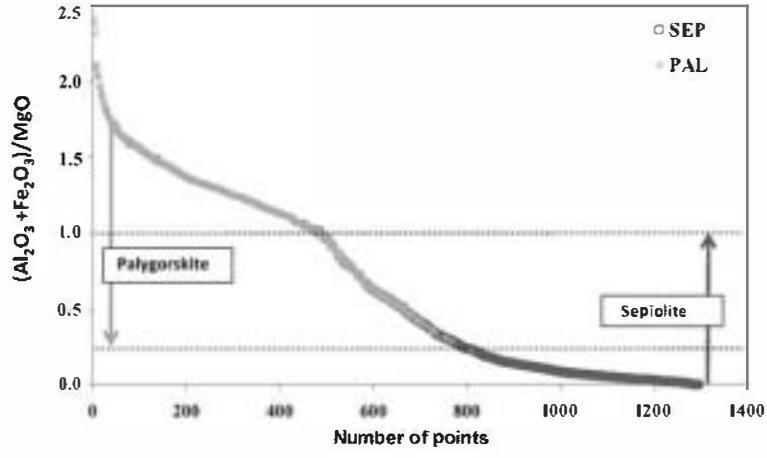

Figure 6. $(Al_2O_3+Fe_2O_3)/MgO$ ratios for all the AEM analyses, ordered from the largest to the smallest values.

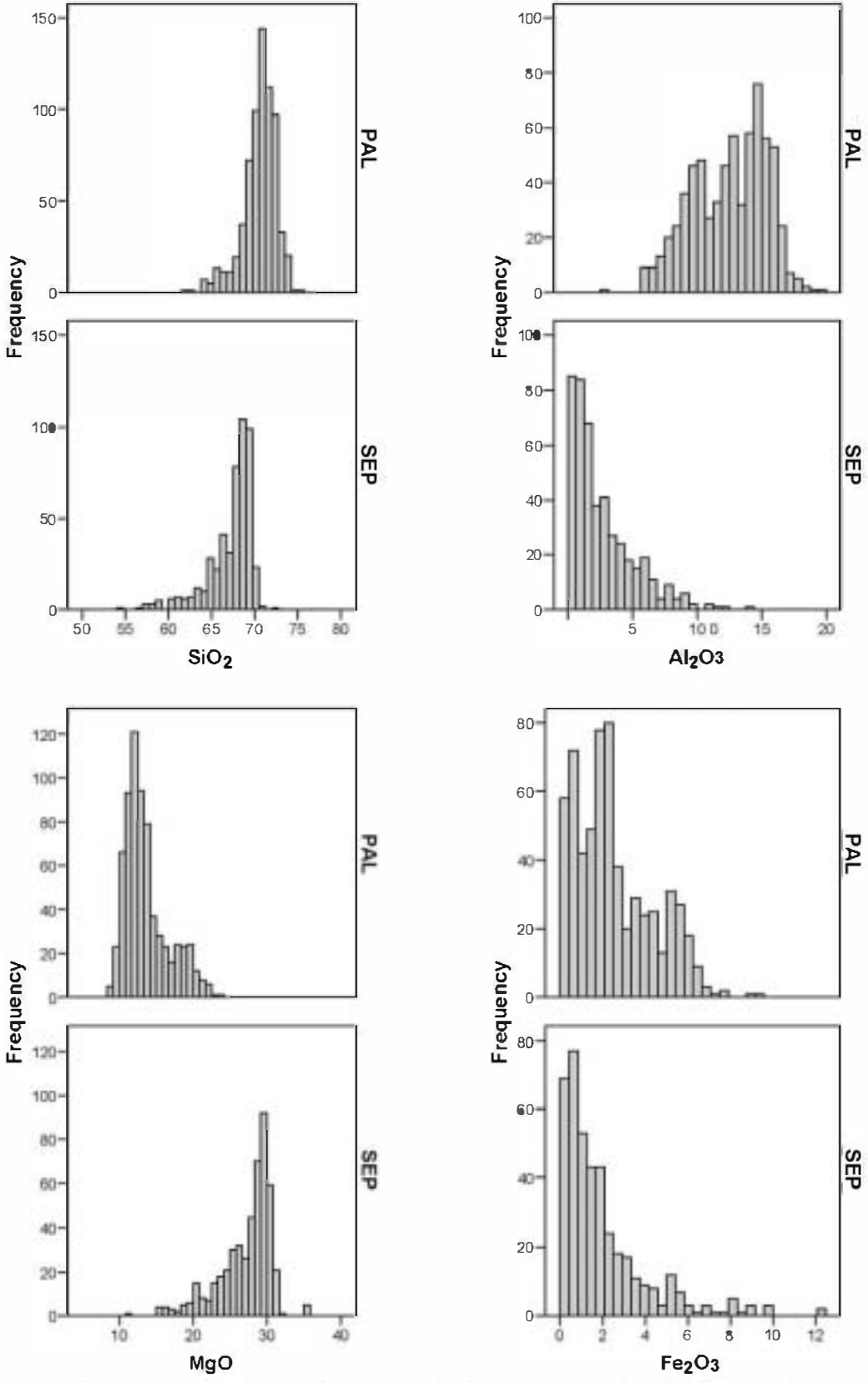

Figure 7. Histograms of the percentages of main oxides of sepiolites and palygorskites studied.

Table 10. Mean values of tetrahedral and octahedral cations, Si/Mg, and R3/R2 for Al-sepiolite samples on the basis of $O_{20}(OH)_2$ (as palygorskite) and for Mg-palygorskite on the basis of $O_{30}(OH)_4$ (as sepiolite).

	Si	^{IV}Al	Στ	^{VI}Al	Fe^{3+}	Mg	Ti	Σo	Ca	K	Na	Si/Mg	R3/R2
E10	12.12	0.03	12.15	1.45	0.21	5.15		6.81	0.06	0.06	0.00	2.35	0.32
E11	12.09	0.06	12.15	1.82	0.26	4.48		6.56	0.09	0.06	0.08	2.70	0.46
TRA	12.23		12.23	1.86	0.24	4.30		6.40	0.07	0.03		2.85	0.49
BAT	7.87	0.18	8.05	0.36	0.13	4.05	0.05	4.59	0.07	0.05	0.02	1.94	0.12
HUN	7.66	0.34	8.01	0.39	0.23	4.01		4.62	0.90	0.15	0.17	1.91	0.15
LIE	7.90	0.10	8.00	0.71	0.21	3.59		4.51	0.05	0.01	0.01	2.20	0.26
POL	7.57	0.42	7.99	0.78	0.43	3.06	0.10	4.37	0.14	0.11		2.47	0.40

e.g. samples POL sepiolite and E10 palygorskite (Tables 4, 5) have similar chemical compositions and as a consequence are projected in the same region of the plot. If histograms corresponding to the main oxides contents (Figure 7) are considered, in all cases both sepiolite and palygorskite fields overlap and sepiolite and palygorskite can contain similar amounts of the four main oxides. No chemical differences exist within a certain number of analyses of sepiolites and palygorskites which have a composition that might be referred to as intermediate. These samples are Mg-palygorskites and Al-sepiolites, the compositions of which are so similar that if the structural formula were fitted as if they were the 'other' mineral (Table 10), fitting sepiolite as palygorskite (with 21 negative charges) and palygorskite as sepiolite (with 32 negative charges), acceptable results from the point of view of occupancy of positions and balance of charges can be reached.

Although slight differences have been found, the analyses indicate a very narrow compositional range in each sample, as illustrated by their small standard deviation. Nevertheless, the samples display a large compositional range from each other. This indicates that each sample has its own features, which may be as a consequence of their different genetic geologic environments. Data from the collection studied here are consistent with those published for these minerals, even taking into account that the literature data can be affected by the presence of impurities. Therefore, a continuous range of chemical composition exists (Figures 1–7) and a compositional gap is absent. On the contrary, chemical compositions can be so similar that a certain degree of polymorphism between Al-sepiolite and Mg-palygorskite exists.

The results obtained raise two questions:

(1) What kinds of conditions are necessary to precipitate sepiolite or palygorskite from a solution with the same composition (with respect to the main oxides)?

(2) What structural arrangements do Al-sepiolite and Mg-palygorskite have? Are the excess Mg and Al within specific domains in the structures or homogeneously distributed along the ribbons?

CONCLUSIONS

Both sepiolite and palygorskite can have a certain degree of tetrahedral substitution (<2% generally).

Theoretical sepiolite has eight octahedral positions, all of which are filled by Mg. Some octahedral substitutions of Mg for Al and/or Fe are possible which induce an increase in the number of octahedral vacancies. Sepiolite can contain large proportions of Al and be considered Al-sepiolite.

Palygorskite has, as is well known, a greater likelihood of octahedral substitution than sepiolite. Al-palygorskite, common palygorskite, Mg-palygorskite, and occasionally Fe-palygorskite also exist.

According to the data presented here, no compositional gap exists between sepiolite and palygorskite.

Al-rich sepiolites and the Mg-rich palygorskites can have similar compositions: Si/Mg between 3.0 and 4.5 and $(Al_2O_3+Fe_2O_3)/MgO$ between 0.25 and 1.

ACKNOWLEDGMENTS

The authors are grateful to Catherine Doyle for checking and improving the English. They are also very grateful to Drs Selahattin Kadir and Yuanfeng Cai whose constructive commets improved the manuscript. Financial support from the Spanish CICYT (project CGL2006-09843) and 'Servicio de Investigación de la U.C.M. (Grupo 910386)' are also acknowledged.

REFERENCES

Akbulut, A. and Kadir, S. (2003) The geology and origin of sepiolite, palygorskite and saponite in Neogene lacustrine sediments of the Serinhisar-Acipayam Basin, Denizli, SW Turkey. *Clays and Clay Minerals*, **51**, 279–292.

Arauzo Perez, A., González López, J.M., and López Aguayo, F. (1989) Primeros datos sobre la mineralogía y génesis del yacimiento de sepiolita de Mara (prov. de Zaragoza). *Boletín de la Sociedad Española de Mineralogía*, **12**, 329–340.

Artioli, G. and Galli, E. (1994) The crystal structures of orthorhombic and monoclinic palygorskite. *Materials Science Forum*, **166–169**, 647–652.

Artioli, G., Galli, E., Burattini, E., Cappuccio, G., and Simeoni, S. (1994) Palygorskite from Bolca, Italy: a characterization by high-resolution synchrotron radiation powder diffraction and computer modelling. *Neues Jahrbuch für Mineralogie Monatshefte*, **5**, 217–229.

Bradley, W.F. (1940) The structural scheme of attapulgite. *American Mineralogist*, **25**, 405–411.

Brauner, K. and Presinger, A. (1956) Struktur und Entstehung des Sepioliths. *Tschermak's Mineralogische und Petrographische Mitteilungen*, **6, 1–2**, pp. 120–140.

Chahi, A., Fritz, B., Duplay, J., Weber, F., and Lucas, J. (1997) Textural transition and genetic relationship between precursor stevensite and sepiolite in lacustrine sediments (Jbel Rhassoul, Morocco). *Clays and Clay Minerals*, **45**, 378–389.

Chahi, A., Petit, S., and Decarreau, A. (2002) Infrared evidence of dioctahedral-trioctahedral site occupancy in palygorskite. *Clays and Clay Minerals*, **50**, 306–313.

Chen, T., Wang, H., Zhang, X., and Zheng, N. (2008) SAED and HRTEM investigation of palygorskite. *Acta Geologica Sinica*, **82**, 385–391.

Chryssikos, G.D., Gionis, V., Kacandes, G.H., Stathopoulou, E.T., Suárez, M., García-Romero, E., and Sánchez del Rio, M. (2009) Octahedral cation analysis of palygorskite by near-infrared spectroscopy. *American Mineralogist*, **94**, 200–203.

Corma, A., Mifsud, A., and Sanz, E. (1987) Influence of the chemical composition and textural characteristics of palygorskite on the acid leaching of octahedral cations. *Clay Minerals*, **22**, 225–232.

Drits, V.A. and Sokolova, G.V. (1971) Structure of palygorskite. *Soviet Physics Crystallography*, **16**, 288–231.

Ece, Ö.I. (1998) Diagenetic transformation of magnesite pebbles and cobbles to sepiolite (meerschaum) in the Miocene Eskişehir lacustrine basin, Turkey. *Clays and Clay Minerals*, **46**, 436–445.

Fahey, J.J., Ross, M., and Axerod, J.M. (1960) Loughlinite, a new hydrous sodium magnesium silicate. *American Mineralogist*, **45**, 270–281.

Galán, E. and Carretero, I. (1999) A new approach to compositional limits for sepiolite and palygorskite. *Clays and Clay Minerals*, **47**, 399–409.

Galán, E., Brell, J.M., La Iglesia, A., and Robertson, R.H.S. (1975) The Caceres palygorskite deposit, Spain. *Proceedings of the International Clay Conference*. Applied Publishing Ltd. Willmette, Illinois 60091, USA, pp. 81–94.

Garcia-Romero, E., Suárez, M., and Bustillo, A. (2004) Characteristics of a Mg-palygorskite in Miocene rocks, Madrid Basin (Spain). *Clays and Clay Minerals*, **52**, 484–494.

García-Romero, E., Suárez, M., Oyarzun, R., López-García, J.A., and Regueiro, M. (2006) Fault-hosted palygorskite from the Serrata de Nijar Deforation Zone (SE Spain). *Clays and Clay Minerals*, **54**, 324–332.

García-Romero, E., Suárez, M., Santaren, J., and Alvarez, A. (2007) Crystallochemical characterization of the palygorskite and sepiolite from the Allou Kagne deposit, Senegal. *Clays and Clay Minerals*, **6**, 606–617.

Gionis, V., Kacandes, G.H., Kastritis, I.D., and Chryssikos, G.D. (2006) On the structure of palygorskite by mid- and near-infrared spectroscopy. *American Mineralogist*, **91**, 1125–1133.

Gionis, V., Kacandes, G.H., Kastritis, I.D., and Chryssikos, G.D. (2007) Combined near-infrared and X-ray diffraction investigation of the octahedral sheet composition of palygorskite. *Clays and Clay Minerals*, **55**, 543–553.

Giusteto, R., Levy, D., and Chiari, G. (2006) Crystal structure refinement of Maya Blue pigment prepared with deuterated indigo, using neutron powder diffraction. *European Journal of Mineralogy*, **18**, 629–640.

Güven, N. (1992) The coordination of aluminum ions in the palygorskite structure. *Clays and Clay Minerals*, **40**, 457–461.

Imai, N. and Otsuka, R. (1984) Sepiolite and palygorskite in Japan. Pp. 211–232 in: *Palygorskite-Sepiolite, Occurrences, Genesis and Uses* (A. Singer and E. Galán, editors). Developments in Sedimentology, **37**, Elsevier, Amsterdam.

Jamoussi, F., Ben Aboud, A., and López-Galindo, A. (2003) Palygorskite genesis through silicate transformation in Tunisian continental Eocene deposits. *Clay Minerals*, **38**, 187–199.

Jones, B.F. and Galán, E. (1991) Sepiolite and palygorskite. Pp. 631–674 in: *Hydrous Phyllosilicates (Exclusive of Micas)* (S.W. Bailey, editor). Reviews in Mineralogy, **19**. Mineralogical Society of America, Washington, D.C.

Kadir, S., Bas, H., and Karakas, Z. (2002) Origin of sepiolite and loughlinite in a Neogene volcano-sedimetary lacustrine environment, Mihaliççik-Eskişehir, Turkey. *The Canadian Mineralogist*, **40**, 1091–1102.

Krekeler, M.P.S. and Guggenheim, S. (2008) Defects in microstructure in palygorskite-sepiolite minerals: A transmission electron microscopy (TEM) study. *Applied Clay Science*, **39**, 98–105.

Li, Z., He, K., Yin, L., Xiong, F., and Zeng, Y.C. (2007) Crystallochemistry of Fe-rich palygorskite from eastern China. *Clay Minerals*, **42**, 453–461.

López-Galindo, A. (1987) Paligorskita en materiales cretácicos de la zona subbetica. Origen. *Boletín de la Sociedad Española de Mineralogía*, **10-2**, 131–139.

López-Galindo, A. and Sánchez Navas, A. (1989) Criterios morfológicos, cristalográficos y geooquímicos de diferenciación entre sepiolitas de origen sedimentario e hidrotermal. *Boletín de la Sociedad Española de Mineralogía*, **12**, 375–383.

López-Galindo, A., Aboud, B., Fenoll Hach-Ali, P., and Casas Ruiz, J. (1996) Mineralogical and geochemical characterization of palygorskite from Gabasa (NE Spain). Evidence of a detrital precursor. *Clay Minerals*, **31**, 33–44.

López-Galindo, A., Fenoll Hach-Alí, P., Pushkarev, A.V., Lytovchenko, A.S., Baker, J.H., and Puskarova, R.A. (2008) Tritium redistribution between water and clay minerals. *Applied Clay Science*, **9**, 151–159.

Lorimer, G.W. and Cliff, G. (1976) Analytical electron microscopy of minerals. Pp. 506–519 in: *Electron Microscopy in Mineralogy* (H.R. Wenk, editor). Springer-Verlag. Berlin.

Magalhaes, C.A., Da Luz, A.B., Baltar, L.M., De Oliveira, C.H., and Becerra, F.J. (2008) Influence of morphology and surface charge on the suitability of palygorskite as drill fluid. *Applied Clay Science*, **42**, 597–600.

Martín-Vivaldi, J.L. and Cano-Ruíz, J. (1956) Contribution to the study of sepiolite: II. Some considerations regarding the mineralogical formula. *Proceedings of four National Conference on Clays and Clay Minerals*. National Academy of Sciences, National Research Council, **156**, 173–176.

Martín-Vivaldi, J.L. and Fenoll, P. (1970) Palygorskites and sepiolites (Hormites). Pp. 553–573 in: *Differential Thermal Analysis* (R.C. Mackenzie, editor). Academic Press, London.

Mumpton, F.A. and Roy, R. (1958) New data on sepiolite and attapulgite. *National Academy of Sciences – National Research Council*, pp. 136–143.

Neaman, A. and Singer, A. (2000) Kinetics of palygorskite hydrolysis in dilute salt solutions. *Clay Minerals*, **35**, 433–441.

Newman, A.C.D. and Brown, G. (1987) The chemical constitution of clays. Pp. 1–129 in: *Chemistry of Clays and Clay Minerals* (A.C.D. Newman, editor). Monograph **6**, Mineralogical Society, London.

Paquet, H., Duplay, J., Valleron-Blanc, M.M., and Millot, G. (1987) Octahedral compositions of individual particles in smectite-palygorskite and smectite-sepiolite assemblages. *Proceedings of the International Clay Conference*. Denver,

1985 (L.G. Schultz, H. Van Olphen, and F.A. Mumpton, editors). The Clay Minerals Society, Bloomington, Indiana, pp. 73–77.

Post, J.L. and Crawford, S. (2007) Varied forms of palygorskite and sepiolite from different geologic systems. *Applied Clay Science*, **26**, 232–244.

Post, J.E. and Heaney, P. J. (2008) Synchrotron powder X-ray diffraction study of the structure and dehydration behavior of palygorskite. *American Mineralogist*, **93**, 667–675.

Rogers, L.E., Quirk, J., and Norrish, K. (1956) Occurrence of an aluminium-sepiolite in a soil having unusual water relationships. *Journal of Soil Science*, **7**, 177–184.

Santaren, J., Sanz, J., and Ruitz-Hitzky, E. (1990) Structural fluorine in sepiolite. *Clays and Clay Minerals*, **38**, 63–68.

Serna, C., Rautureau, M., Prost, R., Tchoubar, C., and Serratosa, J.M. (1977) Etude de la sépiolite a l'aide des données d ela micrsocopie électroniqe, de l'analyse thermopondérale et de la spectroscopie infrarouge. *Bulletin Groupe Française de Argiles*, **XXVI**, 153–163.

Siddiki, M.H.K. (1984) Occurrence of palygorskite in the Deccan Trap formation in India. Pp. 243–250 in: *Palygorskite-Sepiolite, Occurrences, Genesis and Uses* (A. Singer and E. Galán, editors). Developments in Sedimentology, **37**, Elsevier, Amsterdam.

Singer, A. and Norrish, K. (1974) Pedogenic palygorskite occurrences in Australia. *American Mineralogist*, **59**, 508–517.

Singer, A., Stahr, K., and Zarei, M. (1998) Characteristics and origin of sepiolite (Meerschaum) from Central Somalia. *Clay Minerals*, **33**, 349–362.

Springer, G. (1976) Falcondoite, a nickel analogue of sepiolite. *The Canadian Mineralogist*, **14**, 407–408.

Suárez, M. and García-Romero, E. (2006) Macroscopic palygorskite form Lisbom Volcanic Complex. *European Journal of Mineralogy*, **18**, 119–126.

Suárez, M., Robert, M., Elsass, F., and Martín Pozas, J.M. (1994) Evidence of a precursor in the neoformation of palygorskite – new data by analytical electron microscopy. *Clay Minerals*, **29**, 255–264.

Suárez, M., García-Romero, E., and Sánchez del Río, M. (2006) Aproximación a la composición química de la palygorskita a partir de los datos de difracción de rayos-x. *Macla*, **6**, 467–470.

Suárez, M., García-Romero, E., Sánchez del Río, M., Martinetto, P., and Dooryhée, E. (2007) The effect of the octahedral cations on the dimensions of the palygorskite cell. *Clay Minerals*, **42**, 287–297.

Taulet, E., Proenza, J.A., Galí, S., Lewis, J.F., Labrador, M., García-Romero, E., Suárez, M., Longo, F., and Bloise, G. (2009) Ni-sepiolite falcondoite in garnierite mineralization from Falcondo Ni-laterite deposit, Dominica Republic. *Clay Minerals*, **44**, 431–450.

Tien, P.L. (1973) Palygorskite from Warren Quarry, Enderby, Leicestershire, England. *Clay Minerals*, **10**, 27–34.

Torres Ruíz, J., López- Galindo, A., González-López, J.M., and Delgado, A. (1994) Geochemistry of Spanish sepiolite-palygorskite deposits: Genetic considerations based on trace elements and isotopes. *Chemical Geology*, **112**, 221–245.

Verrecchia, E.P. and Le Coustumer, M.N. (1996) Occurrence and genesis of palygorskite and associated clay minerals in a Pleistocene calcrete Complex, Sde Boqer, Negev Desert, Israel. *Clay Minerals*, **31**, 183–202.

Weaver, E. (1984) Origin and geologic implications of the palygorskite deposits of S.E. United States. Pp. 39–58 in: *Palygorskite-Sepiolite, Occurrences, Genesis and Uses* (A. Singer and E. Galán, editors). Developments in Sedimentology, **37**, Elsevier, Amsterdam.

Weaver, C.E. and Polland, L.D. (1973) *The Chemistry of Clay Minerals*. Developments in Sedimentology, Elsevier, Amsterdam, 213 pp.

Yalçin, H. and Bozkaya, Ö. (2004) Ultramafic rock hosted vein sepiolite occurrences in the Ankara ophiolitic mélange, Central Anatolia, Turkey. *Clays and Clay Minerals*, **52**, 227–239.

Zaaboub, N., Abdeljaouad, S., and López-Galindo, A. (2005) Origin of fibrous clays in Tunisian Paleogene continental deposits. *Journal of African Earth Sciences*, **43**, 491–504.